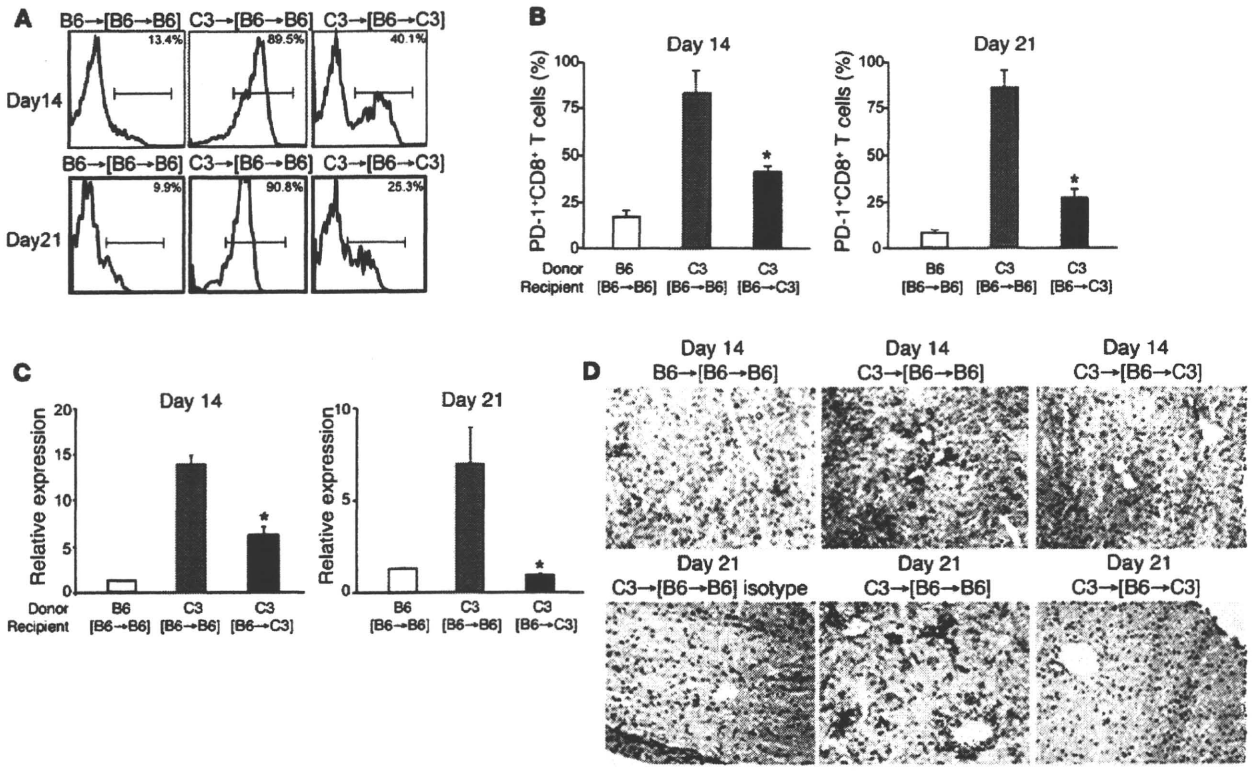

Figure 4
Alloantigen expression on host non-hematopoietic cells stimulates PD-1 and its ligand pathway. [B6→B6] and [B6→C3] chimeras were transplanted as indicated in the legend for Figure 1 (n = 4–8). (**A**) Representative histogram of PD-1 expression among donor CD8$^+$ T cells on day +14 and +21 in syngeneic (left), allogeneic [B6→B6] (middle), and [B6→C3] (right) recipients. (**B**) Frequencies of PD-1$^+$ CD8$^+$ T cells (mean ± SD). (**C**) Relative expressions of *Pdl1* mRNA on day +14 and +21 in the livers of allogeneic [B6→B6] (gray bars) and allogeneic [B6→C3] mice (black bars). Data represent the mean (± SD) of n-fold difference in the amount of *Pdl1* gene expression relative to that in syngeneic mice. (**D**) PD-L1 expression in the liver on day +14 (top row) and +21 (bottom row) from syngeneic (upper left) and allogeneic [B6→B6] (middle) and [B6→C3] (right) recipients. Isotype control of allogeneic [B6→B6] (lower left) is shown. Original magnification, ×200. *P < 0.05 compared with allogeneic controls.

prising observations that alloantigen expression on non-hematopoietic cells inhibited GVL effects but enhanced GVHD. This observation challenges the current paradigm that GVL activity is strongly correlated with the severity of GVHD (1, 2, 27).

We found that alloantigen expression on non-hematopoietic cells induced donor T cell apoptosis and led to a contraction in the size of an alloreactive donor CD8$^+$ T cell pool early after BMT. The remainder of the donor T cells were alive, but their ability to produce cytokines and cytotoxicity were impaired. This defect is similar to T cell exhaustion, which is a principal reason for the inability of the host to eliminate the persisting pathogen in chronic infections (18, 28). CD8$^+$ T cell proliferation and differentiation into cytolytic effectors on an encounter with antigens are variable and change as a consequence of the antigen load (29). As the magnitude of the viral load increases, virus-specific T cells become more functionally impaired. During persistent infection, a high antigen load drives a significant number of virus-specific T cells into activation-induced apoptosis, and the remaining virus-specific T cells remain alive but in a dysfunctional state of cytotoxicity (18, 30–33). In tumor models, antigen quantity determines the behavior of the CD8$^+$ effector cells, including their effector function and sensitivity to apoptosis (34–36). In patients with a larger tumor burden, CD8$^+$ T cells were found to undergo apoptosis (37). Thus, a higher alloantigen load in allogeneic controls as compared with chimeras, in which alloantigen expression is limited to hematopoietic cells and tumor cells, may induce apoptosis and the dysfunction of alloreactive T cells, which leads to the inability of the host to eliminate leukemia.

Our results are consistent with seminal observations by Meunier, Fontaine, and colleagues, who showed that the adoptive transfer of immunodominant mHA (B6^{dom1})-specific T cells eradicates B6^{dom1}-expressing leukemia more efficiently in mice lacking B6^{dom1} expression than in mice expressing B6^{dom1} (38). This was because the widespread expression of B6^{dom1} caused activation-induced apoptosis and dysfunction of donor T cells in mice expressing B6^{dom1} (38, 39). These findings along with our results indicate that allogeneic cellular therapy targeting mHAs exclusively expressed on APCs and tumor cells can induce a potent GVL effect while inducing less-severe GVHD than immunotherapy via targeting of ubiquitously expressed mHAs (40).

The PD-1/PD-L1 pathway is critically involved in T cell exhaustion and tolerance induction in infection and tumor immunology (18–20, 23–25, 41). It is also required for protection against chronic rejection of cardiac allograft, and induction of peripheral dele-

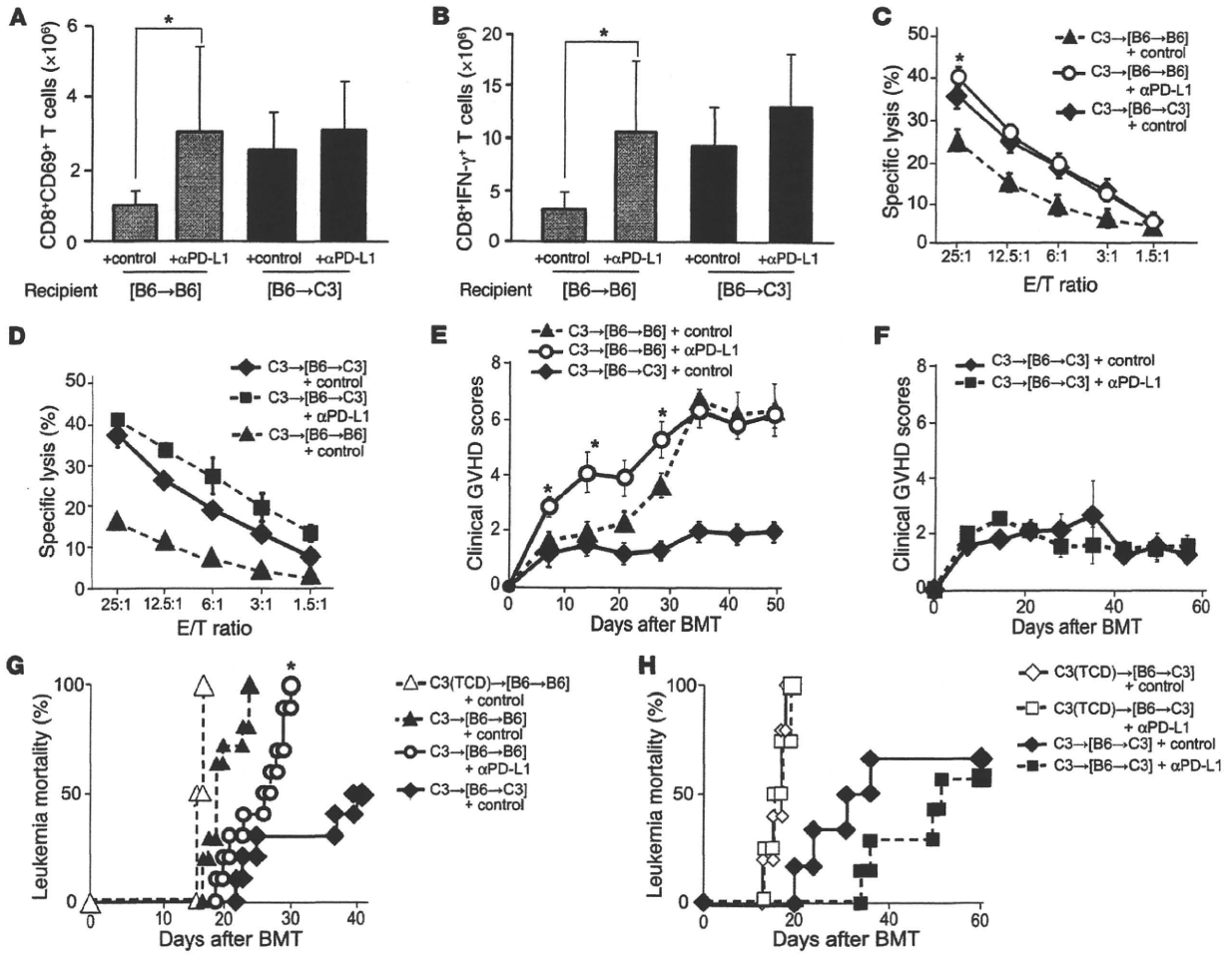

Figure 5

Blockade of the interaction between PD-1 and PD-L1 enhances GVL activity. [B6→C3] and [B6→B6] chimeras were reirradiated and injected with 5 × 10^6 TCD BM cells alone or with 1 × 10^6 $CD8^+$ T cells from C3 donors. Mice were i.p. injected with 500 μg of anti PD-L1 mAbs or controls on day 0 and then 200 μg thereafter on days +3, +6, +9, +12, +15, and +18. Splenocytes were harvested on day +14 to determine the number of $CD8^+CD69^+$ T cells (**A**) and IFN-γ–producing $CD8^+$ T cells (**B**) and CTL activity against EL4 targets (**C** and **D**). Results from a representative experiment of 2 similar experiments (means ± SD, n = 7–8/group). Mean clinical GVHD scores (±SEM) (**E** and **F**) after BMT are shown (n = 5–7/group). (**G** and **H**) Leukemia mortality after BMT in [B6→B6] and [B6→C3] chimeras injected with EL4 cells on day 0 (n = 4–11/group). Data from two similar experiments were combined. αPD-L1, anti–PD-L1 mAbs. *P < 0.05 compared with the corresponding controls.

tional tolerance of alloreactive, anti-donor $CD8^+$ T cells to achieve successful engraftment in BMT (42, 43). In this study, we found that PD-1 expression was upregulated in donor T cells and PD-L1 expression was upregulated in GVHD target organs. The expression of PD-1/PD-L1 was markedly reduced in chimeras lacking alloantigen expression on non-hematopoietic cells. PD-1 and PD-L1 expression is induced upon cell activation and inflammation in GVHD (44); therefore, the absence of alloantigen expression on GVHD target epithelium reduced GVHD in chimeric mice, which resulted in insufficient stimulation of the PD-1/PD-L1 interaction. Target tissue expression of PD-L1 is also critical for the induction of T cell exhaustion or tolerance in chronic viral infection, autoimmune diabetes, and cardiac allografting (19, 42, 45).

Both PD-1 and PD-L1 were markedly upregulated in [B6→B6] mice, but they were also modestly upregulated in [B6→C3] mice. Blockade of PD-1/PD-L1 interactions significantly restored T cell effector functions in [B6→B6] mice but modestly restored them in [B6→C3] mice as well. The relevance of these observations is shown by the PD-1/PD-L1 blockade studies. These data showed that the PD-1/PD-L1 pathway is particularly germane to [B6→B6] mice with widespread expression of alloantigens but also applies, at least in part, to [B6→C3] mice, wherein alloantigen expression is only on APCs. While there is likely to be a role for this pathway in the absence of epithelial alloantigen expression, the full negative impact of this pathway on GVL is only seen when alloantigen expression is present on non-hematopoietic tissues.

Of note, the improvement in GVL by the PD-1/PD-L1 blockade was partial, as has been shown in chronic viral infection (46–48). This may be due to the presence of multiple negative regulatory pathways that contribute to T cell exhaustion, including CTLA-4, IL-10, LAG-3, CD160, and 2B4 (20, 47, 49). In addition, the population of exhausted T cells is heterogeneous, and this interven-

tion is effective only for PD-1^{lo} and not PD-1^{hi}, which are subsets of exhausted T cells (50). Many of these inhibitory receptors are either coexpressed by the same exhausted T cells or differentially expressed on different subsets of exhausted cells. As the severity of the infection increases, the number of different inhibitors expressed per cell increases (47). A second inhibitory receptor, CTLA-4, can be overexpressed by exhausted CD4$^+$ T cells in chronic viral infection, but it appears to have a minimal role on exhausted CD8$^+$ T cells (19, 51). Although CTLA-4 was only slightly upregulated on CD8$^+$ T cells in contrast to the marked upregulation of PD-1 in our CD8-dependent model of MHC-matched BMT, the precise inhibitory receptors of therapeutic interest may differ between CD4$^+$-dependent and CD8$^+$-dependent GVHD/GVL. Another key negative regulatory pathway is mediated by Foxp3$^+$ Tregs. However, enhancement of GVL is not due to effects of the PD-1/PD-L1 blockade on Tregs, because blockade of PD-1/PD-L1 interactions enhances the expansion and function of Tregs (52). The hierarchy of these pathways in regulating GVL will need to be studied in the future based on better understanding of the delineation of T cell subsets and models (53). However, our results suggest the detrimental effect of GVHD-induced immunosuppression on GVL responses, regardless of which inhibitory pathway might be dominant clinically.

In addition, the administration of anti–PD-L1 mAb also exacerbated acute GVHD, as has been shown in a previous study (54). Therefore, the beneficial effects of the PD-1/PD-L1 blockade may be offset by the exacerbation of GVHD. Effects of the inhibitory receptor blockade might depend on the magnitude or stage of donor T cell activation and the severity of GVHD; therefore, the timing and duration of the targeting may be important.

In clinical HSCT, alloantigens continue to be presented on MHC class I in non-hematopoietic cells throughout the lifetime of the transplant recipients. However, a substantial number of patients eventually develop tolerance after resolution of GVHD and often experience leukemia relapse. Although activation-induced apoptosis of alloreactive T cells has been proposed as an explanation of this paradox (55), studies monitoring GVHD-specific T cell clones indicate that host-reactive T cells are continuously present after allogeneic HSCT (56–58). Our results provide a logical explanation for this paradox. However, the process of exhaustion is unlikely to occur in patients not developing GVHD, because induction of T cell exhaustion requires antigen-specific activation of T cells and subsequent differentiation into effector T cells. In these patients, tolerance could be induced by other mechanisms, such as functional central and peripheral tolerance mechanisms. It is well known that GVL is not apparent in patients with high leukemia burden. Although leukemia cells used in the current study do not express PD-L1 (22, 59), leukemia cells expressing PD-L1 may also directly limit the GVL response in patients with high leukemia burden (22, 24, 25). However, such insights from animal models must be extrapolated with caution to clinical studies involving humans.

It has been assumed that T cell exhaustion is antigen specific in chronic viral infection. Bystander lysis of T cells has also been reported in the course of viral infections (60), but is of minimal significance because of its limited magnitude and because normal thymic function can replenish the peripheral T cell pool. In contrast, in GVHD, T cell exhaustion occurs after initial T cell activation and the subsequent development of GVHD. GVHD induces bystander apoptosis of non-host-reactive T cells. In addition, GVHD-mediated injury of the thymus and the secondary lymphoid organs inhibits full replenishment of the peripheral T cell pool (55). Thus, establishment of full immune competence probably requires the additional process of T cell reconstitution following T cell exhaustion.

In conclusion, our results indicated the significance of alloantigen expression on non-hematopoietic cells in GVL. Alloantigen expression on non-hematopoietic cells induces the apoptosis of donor T cells and the dysfunction of cytotoxic effector function, which leads to a reduction in GVL activity. T cell dysfunction was partially restored by blocking PD-1/PD-L1 interactions, which suggests that the therapeutic "tuning" of T cell responses via modulation of negative regulatory pathways represents a novel strategy for enhancing GVL. Our results in combination with those of previous studies (6, 7, 9, 10, 38, 39) provide a complete picture of the effect of alloantigen expression on host APCs, GVHD target epithelium, and tumor cells in allogeneic HSCT; alloantigen expression on host non-hematopoietic cells augments GVHD but suppresses GVL effects. This concept may provide an important framework for understanding the pathophysiology of GVHD and allow for the separation of GVHD and GVL.

Methods

Mice. Female C57BL/6 (B6, H-2^b, CD45.2$^+$), BALB/c (Ba, H-2^d), and DBA/2 (Db, H-2^d) mice were purchased from Charles River Japan. B6.Ly5.1 (H-2^b, CD45.1$^+$) and C3H.Sw (C3, H-2^b) mice were purchased from The Jackson Laboratory. B6-background β_2m-deficient mice ($\beta_2m^{-/-}$: B6.129-β_2-m^{tm1Jae}N12) were purchased from Taconic. The age of mice used ranged from 8 to 12 weeks. Mice were maintained in specific pathogen–free conditions and received normal chaw and hyperchlorinated drinking water for the first 3 weeks after BMT. All experiments involving animals were performed according to a protocol approved by the Institutional Animal Care and Research Advisory Committee of Okayama University and Kyushu University.

Generation of bone marrow chimera and induction of GVHD and GVL. Total body irradiation (TBI: X-ray) was split into 2 doses separated by 4 hours to minimize gastrointestinal toxicity. B6 and C3 mice received 10 Gy TBI, whereas Ba and Db mice received 8.5 Gy TBI. To create BM chimeras, lethally irradiated mice were intravenously injected with 5 × 10^6 TCD BM cells from donors. TCD was performed using anti-CD90 microbeads and AutoMACS (Miltenyi Biotec). Four months later, the chimeric mice were reirradiated and injected with 5 × 10^6 TCD BM cells plus various doses of CD8$^+$ T cells or 2 × 10^6 T cells. T cells and CD8$^+$ T cells were negatively isolated from splenocytes by using a T cell isolation kit and a CD8$^+$ T cell isolation kit (Miltenyi Biotec), respectively, and the AutoMACS. In the GVL experiments, EL4 (H-2^b) derived from a B6 mouse, P815 (H-2^d) derived from a Db mouse, and A20 (H-2^d) derived from a Ba mouse were intravenously injected into BMT recipients on day 0 of BMT. Anti–PD-L1 mAbs were purified from the hybridoma supernatant of clone MIH5 (61), which was a gift from Miyuki Azuma of Tokyo Medical and Dental University, Tokyo, Japan, and i.p. injected at a dose of 500 μg/mouse on day 0, followed by 200 μg/mouse on days +3, +6, +9, +12, +15, and +18 after BMT.

Assessment of GVHD and GVL effects. Survival after BMT was monitored daily, and the degree of clinical GVHD was assessed weekly by using a scoring system that sums changes in 5 clinical parameters: weight loss, posture, activity, fur texture, and skin integrity (maximum index, 10) as described previously (13). The cause of each death after BMT was determined by post mortem examination, and was either GVHD or tumor. The most striking leukemia-specific abnormality induced by EL4, P815, and A20 was macroscopic tumor nodules, marked hepatosplenomegaly, and lower limb paralysis (62). Leukemia death induced by EL4, P815, and A20 was therefore defined by the occurrence of hepatosplenomegaly, macroscopic tumor nodules in the liver

and/or spleen, or hind leg paralysis. GVHD death was defined as the absence of leukemia and by the presence of clinical signs of GVHD, assessed by using a clinical scoring system. Animals surviving beyond the observation period of BMT were sacrificed, and the spleen and liver were harvested for histological evaluation to determine leukemia-free survival.

Flow cytometric analysis. The mAbs used were FITC-, PE-, PerCP-, Cy5.5-, or APC-conjugated anti-mouse CD5.1, CD8, CD45.1, CD45.2, CD69, and PD-1 (BD Biosciences). Cells positive for 7-amino-actinomycin D (BD Biosciences) were excluded from the analysis. For the analysis of donor T cell apoptosis, the cells were stained with Annexin V (MBL). For intracellular IFN-γ staining, the splenocytes were incubated for 4 hours with leukocyte activation cocktail and BD GolgiPlug (BD Biosciences) at 37°C. Then, the cells underwent permeabilization with a BD Cytofix/Cytoperm solution (BD Biosciences) and were stained with FITC-conjugated anti-IFN-γ mAbs (BD Biosciences). For intracellular CTLA-4 staining, cells were stained with PE-conjugated anti-CTLA-4 mAbs (eBioscience). At least 5,000 live events were acquired for the analysis using a FACSCalibur flow cytometer (BD Biosciences).

CTL assay. Splenocytes were removed from chimeric recipients 14 days after BMT, and the mononuclear cells were then separated by density gradient centrifugation. The percentage of $CD8^+$ cells in this fraction was determined by flow cytometry, and counts were normalized for $CD8^+$ cell numbers. Tumor targets, 2×10^6 P815 or EL4, were labeled with 100 μCi of ^{51}Cr sodium salt (Amersham Biosciences) for 2 hours. After washing 3 times, the labeled targets were resuspended in 10% FCS in RPMI and plated at 10^4 cells per well in U-bottom plates (Corning-Costar Corp.). Allogeneic splenocyte preparations, as described above, were added to quadruplicate wells at varying effector-to-target ratios and incubated for 4 hours. Maximal and background release were determined by adding 1% SDS and media alone to the targets, respectively. ^{51}Cr activity in the supernatants collected 4 hours later was determined using a Wallac 1470 WIZARD Gamma Counter (Wallac Oy), and lysis was expressed as a percentage of maximum: percentage of specific lysis = 100 (sample count − background count/maximum count − background count).

Quantitative real-time PCR. Total RNA was isolated from the frozen liver using ISOGEN (Nippon Gene). cDNA was synthesized from 150 μg RNA using a QuantiTect Reverse Transcription Kit (QIAGEN). *Pdl1* mRNA levels were quantified by real-time PCR using the 7500 Real-Time PCR System (Applied Biosystems). TaqMan Universal PCR MasterMix, primers, and the fluorescent TaqMan probe specific for murine PD-L1 (Mm00452054-m1) and a house keeping gene, mGAPDH (Mm99999915-g1), were purchased from Applied Biosystems. The standard was obtained using RNA extracted from syngeneic controls.

Immunohistochemistry. For immunohistochemical analysis, isolated livers were frozen in Tissue-Tek (Sakura Finetek), and 5-μm cryostat sections were prepared. Slides were fixed in 100% acetone and air dried. Endogenous peroxidase activity was blocked with peroxidase blocking reagent (Dako). The sections were incubated with purified rat anti-mouse PD-L1 mAb (clone MIH5; eBiosciences). The primary Abs were detected using the Histofine Simple Stain Mouse MAX PO (Rat) kit and DAB solution (Nichirei). The images were captured using an Olympus BH2 microscope with a Nikon DS-5M color digital camera (Nikon), controlled by Nikon ATC-2U software version 1.5. An Olympus ×10/20 ocular lens and a ×20/0.46 NA objective lens were used. Images were cropped using Adobe Photoshop (Adobe Systems) and were composed using Adobe Illustrator.

Statistics. We used the Kaplan-Meier product-limit method to obtain survival probability and the log-rank test to compare survival curves. The Mann-Whitney *U* test was used to analyze the clinical scores. A *P* value less than 0.05 was considered statistically significant.

Acknowledgments

We thank Miyuki Azuma of Tokyo Medical and Dental University for providing hybridoma MIH5-producing anti-PD-L1 mAbs. This study was supported by grant 21390295 from the Ministry of Education, Culture, Sports, Science, and Technology (Tokyo, Japan) (to T. Teshima), Health and Labor Science Research Grants (Tokyo, Japan) (to T. Teshima), and a grant from the Foundation for Promotion of Cancer Research (Tokyo, Japan) (to T. Teshima).

Received for publication March 11, 2009, and accepted in revised form April 7, 2010.

Address correspondence to: Takanori Teshima, Center for Cellular and Molecular Medicine, Kyushu University Hospital, 3-1-1 Maidashi, Higashi-ku, Fukuoka 812-8582, Japan. Phone: 81.92.642.5947; Fax: 81.92.642.5951; E-mail: tteshima@cancer.med.kyushu-u.ac.jp.

1. Weiden P, et al. Antileukemic effect of graft-versus-host disease in human recipients of allogeneic-marrow grafts. *N Engl J Med.* 1979;300(19):1068–1073.
2. Weiden PL, Sullivan KM, Flournoy N, Storb R, Thomas ED. Antileukemic effect of chronic graft-versus-host disease: contribution to improved survival after allogeneic marrow transplantation. *N Engl J Med.* 1981;304(25):1529–1533.
3. Korngold R, Sprent J. Lethal graft-versus-host disease after bone marrow transplantation across minor histocompatibility barriers in mice. Prevention by removing mature T-cells from marrow. *J Exp Med.* 1978;148(6):1687–1698.
4. Apperley JF, Jones L, Hale G, Goldman JM. Bone marrow transplantation for chronic myeloid leukemia: T-cell depletion with Campath-1 reduces the incidence of acute graft-versus-host disease but may increase the risk of leukemia relapse. *Bone Marrow Transplant.* 1986;1(1):53–66.
5. Atkinson K, et al. Risk factors for chronic graft-versus-host disease after HLA-identical sibling bone marrow transplantation. *Blood.* 1990;75(12):2459–2464.
6. Shlomchik WD, et al. Prevention of graft versus host disease by inactivation of host antigen-presenting cells. *Science.* 1999;285(5426):412–415.
7. Reddy P, Maeda Y, Liu C, Krijanovski OI, Korngold R, Ferrara JL. A crucial role for antigen-presenting cells and alloantigen expression in graft-versus-leukemia responses. *Nat Med.* 2005;11(11):1244–1249.
8. Bleakley M, Riddell SR. Molecules and mechanisms of the graft-versus-leukaemia effect. *Nat Rev Cancer.* 2004;4(5):371–380.
9. Teshima T, et al. Acute graft-versus-host disease does not require alloantigen expression on host epithelium. *Nat Med.* 2002;8(6):575–581.
10. Jones SC, Murphy GF, Friedman TM, Korngold R. Importance of minor histocompatibility antigen expression by nonhematopoietic tissues in a CD4+ T cell-mediated graft-versus-host disease model. *J Clin Invest.* 2003;112(12):1880–1886.
11. Ruggeri L, et al. Effectiveness of donor natural killer cell alloreactivity in mismatched hematopoietic transplants. *Science.* 2002;295(5562):2097–2100.
12. Matte CC, et al. Donor APCs are required for maximal GVHD but not for GVL. *Nat Med.* 2004;10(9):987–992.
13. Cooke KR, et al. An experimental model of idiopathic pneumonia syndrome after bone marrow transplantation. I. The roles of minor H antigens and endotoxin. *Blood.* 1996;88(8):3230–3239.
14. Korngold R, Sprent J. Features of T cells causing H-2-restricted lethal graft-vs.-host disease across minor histocompatibility barriers. *J Exp Med.* 1982;155(3):872–883.
15. Zhang Y, Joe G, Hexner E, Zhu J, Emerson SG. Alloreactive memory T cells are responsible for the persistence of graft-versus-host disease. *J Immunol.* 2005;174(5):3051–3058.
16. Stefanova I, Dorfman JR, Germain RN. Self-recognition promotes the foreign antigen sensitivity of naive T lymphocytes. *Nature.* 2002;420(6914):429–434.
17. Zhang Y, Louboutin JP, Zhu J, Rivera AJ, Emerson SG. Preterminal host dendritic cells in irradiated mice prime CD8+ T cell-mediated acute graft-versus-host disease. *J Clin Invest.* 2002;109(10):1335–1344.
18. Zajac AJ, et al. Viral immune evasion due to persistence of activated T cells without effector function. *J Exp Med.* 1998;188(12):2205–2213.
19. Barber DL, et al. Restoring function in exhausted CD8 T cells during chronic viral infection. *Nature.* 2006;439(7077):682–687.
20. Shin H, Wherry EJ. CD8 T cell dysfunction during chronic viral infection. *Curr Opin Immunol.* 2007;19(4):408–415.
21. Keir ME, Butte MJ, Freeman GJ, Sharpe AH. PD-1 and its ligands in tolerance and immunity. *Annu Rev Immunol.* 2008;26:677–704.
22. Dong H, et al. Tumor-associated B7-H1 promotes T-cell apoptosis: a potential mechanism of immune evasion. *Nat Med.* 2002;8(8):793–800.
23. Ahmadzadeh M, et al. Tumor antigen-specific CD8

T cells infiltrating the tumor express high levels of PD-1 and are functionally impaired. *Blood.* 2009; 114(8):1537–1544.
24. Zhang L, Gajewski TF, Kline J. PD-1/PD-L1 interactions inhibit anti-tumor immune responses in a murine acute myeloid leukemia model. *Blood.* 2009; 114(8):1545–1552.
25. Mumprecht S, Schurch C, Schwaller J, Solenthaler M, Ochsenbein AF. PD-1 signaling on chronic myeloid leukemia-specific T cells results in T cell exhaustion and disease progression. *Blood.* 2009; 114(8):1528–1536.
26. Iwai Y, Terawaki S, Ikegawa M, Okazaki T, Honjo T. PD-1 inhibits antiviral immunity at the effector phase in the liver. *J Exp Med.* 2003;198(1):39–50.
27. Horowitz MM, et al. Graft-versus-leukemia reactions after bone marrow transplantation. *Blood.* 1990;75(3):555–562.
28. Gallimore A, et al. Induction and exhaustion of lymphocytic choriomeningitis virus-specific cytotoxic T lymphocytes visualized using soluble tetrameric major histocompatibility complex class I-peptide complexes. *J Exp Med.* 1998;187(9):1383–1393.
29. Welsh RM. Assessing CD8 T cell number and dysfunction in the presence of antigen. *J Exp Med.* 2001; 193(5):F19–F22.
30. Moskophidis D, Lechner F, Pircher H, Zinkernagel RM. Virus persistence in acutely infected immunocompetent mice by exhaustion of antiviral cytotoxic effector T cells. *Nature.* 1993;362(6422):758–761.
31. Appay V, et al. HIV-specific CD8(+) T cells produce antiviral cytokines but are impaired in cytolytic function. *J Exp Med.* 2000;192(1):63–75.
32. Xiong Y, et al. Simian immunodeficiency virus (SIV) infection of a rhesus macaque induces SIV-specific CD8(+) T cells with a defect in effector function that is reversible on extended interleukin-2 incubation. *J Virol.* 2001;75(6):3028–3033.
33. Pantaleo G, Harari A. Functional signatures in antiviral T-cell immunity for monitoring virus-associated diseases. *Nat Rev Immunol.* 2006;6(5):417–423.
34. Tham EL, Mescher MF. Signaling alterations in activation-induced nonresponsive CD8 T cells. *J Immunol.* 2001;167(4):2040–2048.
35. Tham EL, Shrikant P, Mescher MF. Activation-induced nonresponsiveness: a Th-dependent regulatory checkpoint in the CTL response. *J Immunol.* 2002;168(3):1190–1197.
36. Boissonnas A, et al. Antigen distribution drives programmed antitumor CD8 cell migration and determines its efficiency. *J Immunol.* 2004;173(1):222–229.
37. Saito T, Dworacki G, Gooding W, Lotze MT, Whiteside TL. Spontaneous apoptosis of CD8+ T lymphocytes in peripheral blood of patients with advanced melanoma. *Clin Cancer Res.* 2000;6(4):1351–1364.
38. Fontaine P, Roy-Proulx G, Knafo L, Baron C, Roy DC, Perreault C. Adoptive transfer of minor histocompatibility antigen-specific T lymphocytes eradicates leukemia cells without causing graft-versus-host disease. *Nat Med.* 2001;7(7):789–794.
39. Meunier MC, Roy-Proulx G, Labrecque N, Perreault C. Tissue distribution of target antigen has a decisive influence on the outcome of adoptive cancer immunotherapy. *Blood.* 2003;101(2):766–770.
40. Dickinson AM, et al. In situ dissection of the graft-versus-host activities of cytotoxic T cells specific for minor histocompatibility antigens. *Nat Med.* 2002; 8(4):410–414.
41. Ding ZC, Blazar BR, Mellor AL, Munn DH, Zhou G. Chemotherapy rescues tumor-driven aberrant CD4+ T-cell differentiation and restores an activated polyfunctional helper phenotype. *Blood.* 2010; 115(12):2397–2406.
42. Tanaka K, et al. PDL1 is required for peripheral transplantation tolerance and protection from chronic allograft rejection. *J Immunol.* 2007; 179(8):5204–5210.
43. Haspot F, et al. Peripheral deletional tolerance of alloreactive CD8 but not CD4 T cells is dependent on the PD-1/PD-L1 pathway. *Blood.* 2008; 112(5):2149–2155.
44. Yamazaki T, et al. Expression of programmed death 1 ligands by murine T cells and APC. *J Immunol.* 2002;169(10):5538–5545.
45. Keir ME, et al. Tissue expression of PD-L1 mediates peripheral T cell tolerance. *J Exp Med.* 2006; 203(4):883–895.
46. Crawford A, Wherry EJ. The diversity of costimulatory and inhibitory receptor pathways and the regulation of antiviral T cell responses. *Curr Opin Immunol.* 2009;21(2):179–186.
47. Blackburn SD, et al. Coregulation of CD8+ T cell exhaustion by multiple inhibitory receptors during chronic viral infection. *Nat Immunol.* 2009; 10(1):29–37.
48. Petrovas C, et al. PD-1 is a regulator of virus-specific CD8+ T cell survival in HIV infection. *J Exp Med.* 2006;203(10):2281–2292.
49. Brooks DG, Trifilo MJ, Edelmann KH, Teyton L, McGavern DB, Oldstone MB. Interleukin-10 determines viral clearance or persistence in vivo. *Nat Med.* 2006;12(11):1301–1309.
50. Blackburn SD, Shin H, Freeman GJ, Wherry EJ. Selective expansion of a subset of exhausted CD8 T cells by alphaPD-L1 blockade. *Proc Natl Acad Sci U S A.* 2008;105(39):15016–15021.
51. Kaufmann DE, et al. Upregulation of CTLA-4 by HIV-specific CD4+ T cells correlates with disease progression and defines a reversible immune dysfunction. *Nat Immunol.* 2007;8(11):1246–1254.
52. Franceschini D, et al. PD-L1 negatively regulates CD4+CD25+Foxp3+ Tregs by limiting STAT-5 phosphorylation in patients chronically infected with HCV. *J Clin Invest.* 2009;119(3):551–564.
53. Socie G, Blazar BR. Acute graft-versus-host disease: from the bench to the bedside. *Blood.* 2009; 114(20):4327–4336.
54. Blazar BR, et al. Blockade of programmed death-1 engagement accelerates graft-versus-host disease lethality by an IFN-gamma-dependent mechanism. *J Immunol.* 2003;171(3):1272–1277.
55. Brochu S, Rioux-Masse B, Roy J, Roy DC, Perreault C. Massive activation-induced cell death of alloreactive T cells with apoptosis of bystander postthymic T cells prevents immune reconstitution in mice with graft-versus-host disease. *Blood.* 1999;94(2):390–400.
56. Dey B, et al. The fate of donor T-cell receptor transgenic T cells with known host antigen specificity in a graft-versus-host disease model. *Transplantation.* 1999;68(1):141–149.
57. Choi EY, et al. Real-time T-cell profiling identifies H60 as a major minor histocompatibility antigen in murine graft-versus-host disease. *Blood.* 2002; 100(13):4259–4265.
58. Michalek J, Collins RH, Hill BJ, Brenchley JM, Douek DC. Identification and monitoring of graft-versus-host specific T-cell clone in stem cell transplantation. *Lancet.* 2003;361(9364):1183–1185.
59. Hirano F, et al. Blockade of B7-H1 and PD-1 by monoclonal antibodies potentiates cancer therapeutic immunity. *Cancer Res.* 2005;65(3):1089–1096.
60. Ando K, et al. Perforin, Fas/Fas ligand, and TNF-alpha pathways as specific and bystander killing mechanisms of hepatitis C virus-specific human CTL. *J Immunol.* 1997;158(11):5283–5291.
61. Tsushima F, et al. Preferential contribution of B7-H1 to programmed death-1-mediated regulation of hapten-specific allergic inflammatory responses. *Eur J Immunol.* 2003;33(10):2773–2782.
62. Teshima T, et al. IL-11 separates graft-versus-leukemia effects from graft-versus-host disease after bone marrow transplantation. *J Clin Invest.* 1999;104(3):317–325.

Published January 31, 2011

JEM

Article

The Wnt agonist R-spondin1 regulates systemic graft-versus-host disease by protecting intestinal stem cells

Shuichiro Takashima,[1] Masanori Kadowaki,[1] Kazutoshi Aoyama,[1] Motoko Koyama,[1] Takeshi Oshima,[3] Kazuma Tomizuka,[3] Koichi Akashi,[1,2] and Takanori Teshima[2]

[1]Department of Medicine and Biosystemic Science and [2]Center for Cellular and Molecular Medicine, Kyushu University Graduate School of Medical Science, Higashi-ku, Fukuoka 812-8582, Japan
[3]Innovative Drug Research Laboratories, Kyowa Hakko Kirin Co., Ltd., Machida, Tokyo 194-8533, Japan

Graft-versus-host disease (GVHD) is a major complication of allogeneic bone marrow transplantation (BMT), and damage to the gastrointestinal (GI) tract plays a critical role in amplifying systemic disease. Intestinal stem cells (ISCs) play a pivotal role not only in physiological tissue renewal but also in regeneration of the intestinal epithelium after injury. In this study, we have discovered that pretransplant conditioning regimen damaged ISCs; however, the ISCs rapidly recovered and restored the normal architecture of the intestine. ISCs are targets of GVHD, and this process of ISC recovery was markedly inhibited with the development of GVHD. Injection of Wnt agonist R-spondin1 (R-Spo1) protected against ISC damage, enhanced restoration of injured intestinal epithelium, and inhibited subsequent inflammatory cytokine cascades. R-Spo1 ameliorated systemic GVHD after allogeneic BMT by a mechanism dependent on repair of conditioning-induced GI tract injury. Our results demonstrate for the first time that ISC damage plays a central role in amplifying systemic GVHD; therefore, we propose ISC protection by R-Spo1 as a novel strategy to improve the outcome of allogeneic BMT.

CORRESPONDENCE
Takanori Teshima:
tteshima@
cancer.med.kyushu-u.ac.jp

Abbreviations used: BMT, BM transplantation; GI, gastrointestinal; GVHD, graft-versus-host disease; ISC, intestinal stem cell; R-Spo1, R-spondin1; SCT, stem cell transplantation; TBI, total body irradiation; TCD, T cell depleted.

An important aspect of cancer therapy is maintaining a fine balance between the use of chemoradiotherapy doses high enough to kill tumor cells and doses low enough to prevent damage to normal tissue. The gastrointestinal (GI) epithelium and BM are the most rapidly self-renewing tissues in adults and are therefore susceptible to cytotoxic exposure, showing a rapid expression of damage. Damage to these tissues is a dose-limiting and potentially lethal toxicity of chemoradiotherapy used to treat cancer patients. Allogeneic hematopoietic stem cell transplantation (SCT) is a curative therapy for hematologic malignancies that works by delivering healthy hematopoietic stem cells to replace BM destroyed by the high-dose chemoradiotherapy (pretransplant conditioning); however, this process is complicated by regimen-related toxicity against other tissues, particularly in the GI tract.

Graft-versus-host disease (GVHD), a major and devastating complication of allogeneic SCT, is a complex process involving donor T cell responses to host antigens and the dysregulation of inflammatory cytokine cascades (Hill et al., 1997; Hill and Ferrara, 2000; Teshima et al., 2002a; Ferrara et al., 2003). Increasing evidence from experimental and clinical SCT suggests that conditioning-mediated GI tract damage plays a central role in amplifying GVHD by propagating its cytokine storm characteristics (Hill et al., 1997; Hill and Ferrara, 2000; Ferrara et al., 2003). Intestinal epithelial cells are continuously regenerated from intestinal stem cells (ISCs), which are key to the regeneration of damaged intestinal epithelium (Batlle et al., 2002; Pinto et al., 2003; Barker et al., 2007, 2008). However, the dynamic process of damage and repopulation of ISCs, which play a pivotal

The Rockefeller University Press $30.00
J. Exp. Med. Vol. 208 No. 2 285-294
www.jem.org/cgi/doi/10.1084/jem.20101559

Supplemental Material can be found at:
http://jem.rupress.org/content/suppl/2011/01/31/jem.20101559.DC1.html

Published January 31, 2011

role in the competitive race between tissue damage and restoration during conditioning regimens and GVHD, is not well understood.

Wnt signaling plays a critical role in the regulation of intestinal epithelial cell proliferation during their maturation or regeneration (Batlle et al., 2002; Pinto et al., 2003; Reya and Clevers, 2005; Barker et al., 2008). R-spondin1 (R-Spo1) is a potent activator of the Wnt signaling pathway. It relieves the Dickkopf-1 inhibition imposed on the Wnt signaling pathway and thereby increases levels of the Wnt pathway coreceptor low-density lipoprotein receptor–related protein-6 on cell surface (Kim et al., 2005; Binnerts et al., 2007). We have previously shown that human R-Spo1 transgenic mice had a marked thickening of the mucosa and displayed crypt epithelial hyperplasia (Kim et al., 2005). Injection of human R-Spo1 induced rapid onset of crypt cell proliferation in the intestine of normal mice through β-catenin stabilization and subsequent transcriptional activation of target genes (Kim et al., 2005). Thus, injection of R-Spo1 protected mice from chemotherapy- or radiation-induced colitis by stimulating mucosal regeneration and restoring intestinal architecture (Kim et al., 2005; Zhao et al., 2007, 2009; Bhanja et al., 2009). However, because of the lack of specific markers for ISCs, it is unclear whether this result was mediated by the direct effect of R-Spo1 on ISCs.

In this study, we investigated the dynamic process of ISC damage and repopulation during the pretransplant conditioning regimen, total body irradiation (TBI), and GVHD. The effects of R-Spo1 on this process were also examined using recently identified markers for ISCs such as *Lgr5* (*leucine-rich repeat–containing G protein–coupled receptor 5*) and *Olfm4* (*Olfactomedin-4*; Barker et al., 2007, 2008; van der Flier et al., 2009a,b). *Lgr5* and *Olfm4* mark rapidly cycling crypt base columnar cells, which can give rise to all intestinal epithelial lineages (Barker et al., 2007, 2008; van der Flier et al., 2009a,b). We then tested the hypothesis that protection of ISCs improves the outcome of allogeneic SCT by regulating systemic GVHD using a well-characterized murine model of MHC-mismatched, haploidentical BM transplantation (BMT).

RESULTS

R-Spo1 protected against radiation-induced colitis by stimulating proliferation of ISCs through the Wnt signaling pathway

We first studied the effect of R-Spo1 on the expression of Wnt target genes in the small intestine using quantitative real-time PCR. Injection of R-Spo1 (200 μg/day) over 3 d significantly up-regulated the expression of Wnt target genes, including *Axin2*, *Ascl2* (*Achaete scute-like 2*), and *Lgr5* (Fig. S1 A). We noted an elongation of villi with an increased number of *Olfm4*$^+$ ISCs in the crypts of R-Spo1–treated animals (Fig. S1, B and C). Ki-67 immunostaining also showed crypt hyperplasia paralleling an increased number of Ki-67$^+$ cycling cells in the crypts (Fig. S1, D and E).

Next, we evaluated the effect of R-Spo1 administration on the process of mucosal regeneration after TBI. According to our preliminary experiments (unpublished data), mice irradiated with 15 Gy TBI on day 0 were intravenously injected with 200 μg R-Spo1 once daily from day −3 to −1 and from day 1–3. The real-time PCR analysis of the small intestine harvested 6 h after the final administration of R-Spo1 showed up-regulated expression of *Axin2* and *Ascl2* in R-Spo1–treated mice (Fig. 1 A). The *Olfm4*$^+$ cell population was significantly greater in R-Spo1–treated mice than in controls on day 3 (Fig. 1, B and C); as a result, radiation colitis characterized

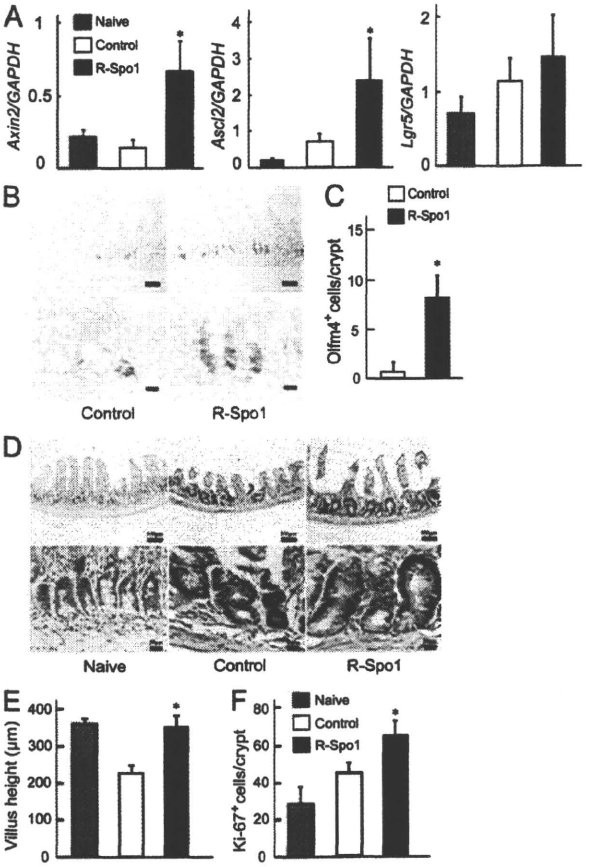

Figure 1. R-Spo1 protected against radiation-induced colitis by enhancing proliferation of ISCs via the Wnt signaling pathway. B6D2F1 mice irradiated with 15 Gy TBI on day 0 and intravenously injected with R-Spo1 (200 μg/day) or control from day −3 to −1 and day 1–3. The small intestine was harvested 6 h after the final administration of R-Spo1 for quantitative real-time PCR analysis and in situ hybridization, and 24 h later for immunohistochemistry. (A) Quantitative real-time PCR analysis of *Axin2*, *Ascl2*, and *Lgr5* transcripts normalized to those of GAPDH (naive, $n = 3$; control, $n = 4$; R-Spo1, $n = 4$). (B) In situ hybridization for *Olfm4* on representative crypts. (C) Quantification of *Olfm4*$^+$ cells per crypt ($n = 4$ per group). (D) Ki-67 staining of the terminal ileum. (E) Villus height of the terminal ileum (naive, $n = 3$; control, $n = 4$; R-Spo1, $n = 4$). (F) Quantification of Ki-67$^+$ cells per crypt (naive, $n = 3$; control, $n = 4$; R-Spo1, $n = 4$). Data are representative of two independent experiments and are shown as means ± SD. *, $P < 0.05$ compared with control. Bars: (B and D, top row) 100 μm; (B and D, bottom row) 20 μm.

Published January 31, 2011

by blunting of villi was significantly reduced in R-Spo1–treated animals (Fig. 1, D and E). We also noted crypt hyperplasia and an increased number of Ki-67$^+$ cycling cells in the crypt on day 4 (Fig. 1, D and F). These results extend our previous observations regarding R-Spo1–mediated mitogenic effects on the intestinal epithelium (Kim et al., 2005) by documenting the effects of R-Spo1 on ISCs.

R-Spo1 protected against ISC damage after allogeneic BMT

GI tract damage is much more severe in allogeneic SCT than in autologous or syngeneic SCT because of the additional detrimental effects of GVHD on the GI tract. However, it remains to be elucidated whether GVHD targets ISCs that are crucial for the regeneration of damaged intestinal epithelium and also how the damage and repopulation of ISCs affects the process of mucosal injury and regeneration after allogeneic BMT. To address these issues, lethally irradiated B6D2F1 mice were transplanted with 5 × 10^6 T cell–depleted (TCD) BM cells with or without 2 × 10^6 T cells from MHC-mismatched C57BL/6 (B6) or B6-Ly5.1 donors on day 0. Small intestines were harvested from mice on day 0 before TBI and on days 3 and 6 after BMT, and quantitative real-time PCR and in situ hybridization were performed to determine the kinetics of loss and repopulation of *Olfm4*$^+$ ISCs. R-Spo1 was injected from day −3 to −1 and day 1–3 after BMT. TCD animals and control-treated allogeneic animals served as non-GVHD

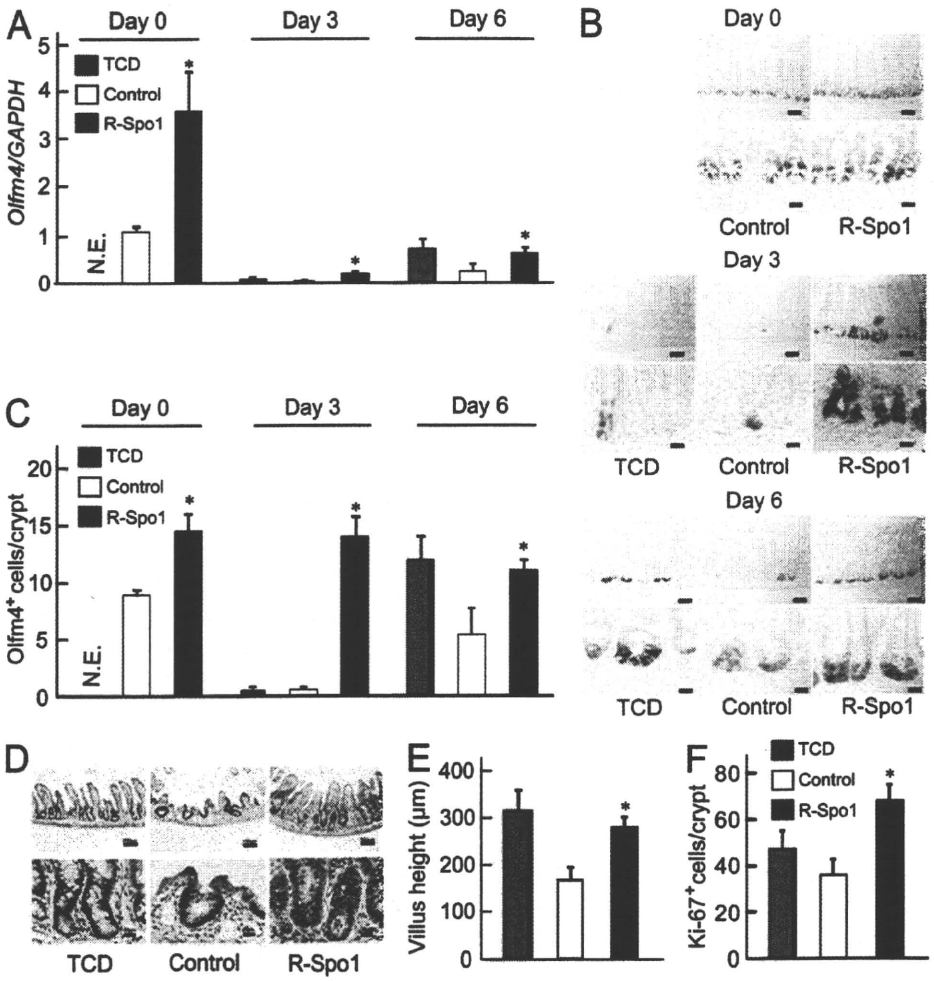

Figure 2. R-Spo1 enhanced repopulation of ISCs after allogeneic BMT. Lethally irradiated B6D2F1 mice were transplanted with 5 × 10^6 TCD BM with or without 2 × 10^6 T cells from B6 donors on day 0. R-Spo1 (200 μg/day) or control was intravenously injected from day −3 to −1 and day 1–3 after BMT. Small intestines were harvested on day 0 (before TBI) and days 3 and 6. (A) Quantitative real-time PCR analysis of *Olfm4* transcripts normalized to those of GAPDH (TCD, $n = 3$; control, $n = 4$; R-Spo1, $n = 4$ per time point). (B) In situ hybridization of *Olfm4* on representative crypts. (C) Quantification of *Olfm4*$^+$ cells per crypt (TCD, $n = 3$; control, $n = 4$; R-Spo1, $n = 4$ per time point). (D) Ki-67 staining of the terminal ileum harvested on day 6. (E) Villus height of the terminal ileum was measured as described in Fig. 1 E using the slides in D (TCD, $n = 3$; control, $n = 5$; R-Spo1, $n = 5$). (F) Quantification of Ki-67$^+$ cells per crypt (TCD, $n = 3$; control, $n = 5$; R-Spo1, $n = 5$). Data are representative of two independent experiments and are shown as means ± SD. *, $P < 0.05$ compared with control. Bars: (B and D, top rows) 100 μm; (B and D, bottom rows) 20 μm.

Published January 31, 2011

controls and GVHD controls, respectively. In both groups, *Olfm4* expression levels significantly decreased in the small intestine on day 3 (Fig. 2 A). In TCD animals, *Olfm4* expression recovered to normal levels on day 6, whereas in allogeneic controls, it remained low. In contrast, *Olfm4* expression levels in R-Spo1–treated animals were significantly higher on and after day 0 in comparison with allogeneic controls (Fig. 2 A). These results were further confirmed by in situ hybridization analysis of *Olfm4* transcripts in the small intestine. The *Olfm4*$^+$ ISC population significantly decreased in both TCD and allogeneic controls on day 3 (Fig. 2, B and C). On day 6, *Olfm4*$^+$ cells were fully repopulated in TCD animals, and their numbers were significantly higher than their numbers in allogeneic controls. These results demonstrate that TBI injures ISCs and that the process of ISC repopulation is inhibited in GVHD. In R-Spo1–treated animals, the number of *Olfm4*$^+$ cells was consistently higher before and after BMT than that in allogeneic controls. Villous atrophy was severe in allogeneic controls on day 6, whereas injection of R-Spo1 resulted in crypt hyperplasia with an increased number of Ki-67$^+$ cycling cells in the crypts and dramatically ameliorated GI tract damage (Fig. 2, D–F). R-Spo1 treatment before TBI thus expanded the ISC pool and minimized intestinal damage.

R-Spo1 suppressed inflammatory cytokine cascades and donor T cell activation after allogeneic BMT

We then tested the hypothesis that protection of ISCs against TBI regulates systemic GVHD and improves the outcome of

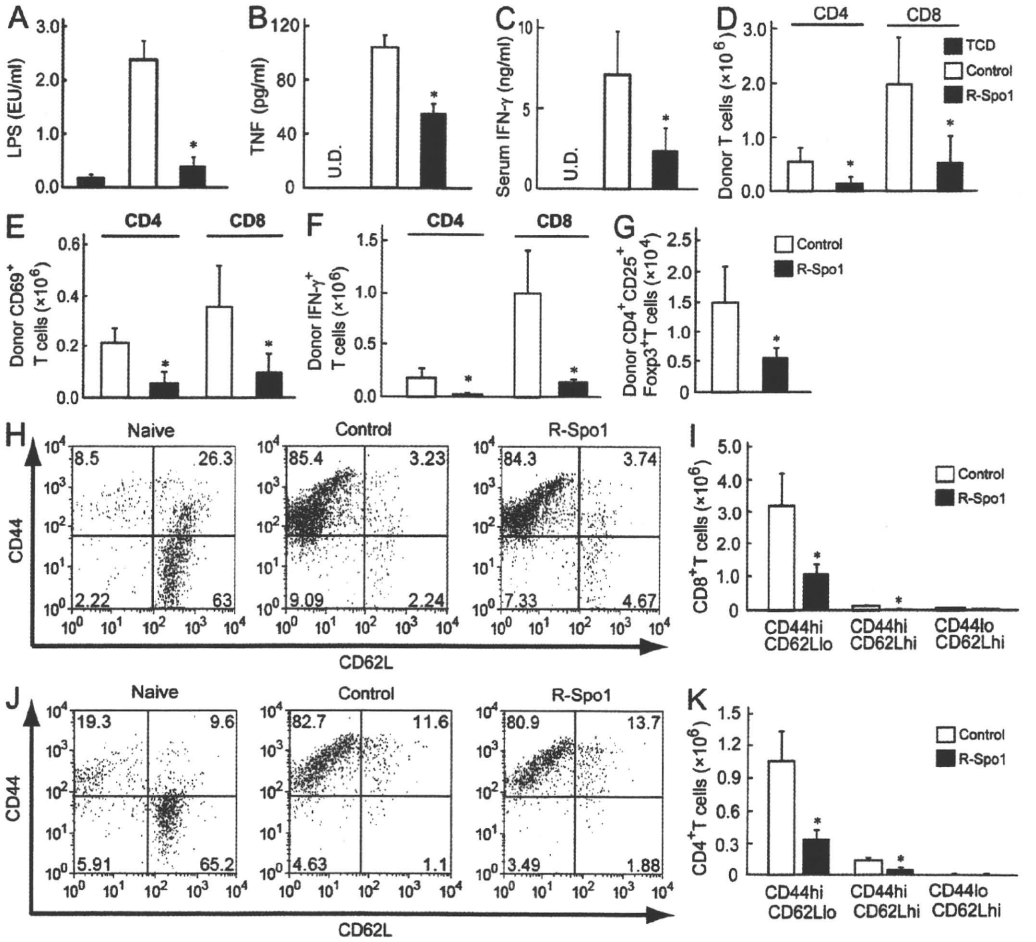

Figure 3. R-Spo1 regulated activation of inflammatory and cellular effectors in GVHD. Lethally irradiated B6D2F1 mice were transplanted with 5 × 10^6 TCD BM cells with or without 2 × 10^6 T cells from B6-Ly5.1 (CD45.1$^+$) donors on day 0. R-Spo1 (200 µg/day) or control was intravenously injected from day −3 to −1 and day 1–3 after BMT. Serum samples and splenocytes were obtained 5–7 d after BMT (TCD, n = 3; control, n = 5; R-Spo1, n = 5). (A–C) Serum levels of LPS (A), TNF (B), and IFN-γ (C) are shown. (D–G) Numbers of donor (CD45.1$^+$) T cells (D), CD69$^+$ donor T cells (E), IFN-γ$^+$ donor T cells (F), and CD4$^+$CD25$^+$Foxp3$^+$ T reg cells (G) in spleen are shown. (H–K) Flow cytometric analysis and enumeration of T cell subsets in spleen. Numbers represent the percentage of cells in the dot plot quadrants. CD8$^+$ T cells (H and I) and CD4$^+$ T cells (J and K) are shown. Data are representative of two independent experiments and are shown as means ± SD. *, $P < 0.05$ compared with control. U.D., undetectable.

Published January 31, 2011

allogeneic SCT. Serum LPS levels are increased during GVHD and correlate with GI tract damage (Hill et al., 1997; Hill and Ferrara, 2000; Ferrara et al., 2003). LPS has been shown to stimulate production of excessive inflammatory cytokines such as TNF that are implicated in the pathogenesis of GVHD (Nestel et al., 1992; Hill et al., 1997; Hill and Ferrara, 2000; Cooke et al., 2001; Teshima et al., 2002a; Ferrara et al., 2003). LPS and TNF levels were markedly increased in allogeneic controls but were significantly reduced in R-Spo1–treated animals (Fig. 3, A and B), suggesting that the fortification of GI mucosal barrier functions by R-Spo1 suppresses subsequent inflammatory cascades in GVHD. We also investigated the effect of R-Spo1 on allogeneic donor T cell responses. Serum levels of IFN-γ, a hallmark of systemic T cell responses in GVHD, were significantly lower in R-Spo1–treated mice than in controls (Fig. 3 C). Donor T cell expansion (Fig. 3 D) and activation, as determined by CD69 expression (Fig. 3 E), and intracellular IFN-γ (Fig. 3 F) were also significantly reduced in R-Spo1–treated mice. Recent studies have shown that Wnt signaling can modulate adoptive immunity by enhancing regulatory T cell (T reg cell) survival and inducing $CD4^+$ T cell anergy, as well as by regulating effector $CD8^+$ T cell development and promoting memory $CD8^+$ T cell generation (Ding et al., 2008; Gattinoni et al., 2009). However, in our study, the number of $CD4^+CD25^+Foxp3^+$ T reg cells in the spleen was significantly less in R-Spo1–treated mice than in controls (Fig. 3 G), and the ratios of effector to memory $CD8^+$ (Fig. 3, H and I) and $CD4^+$ T cells (Fig. 3, J and K) were similar between R-Spo1–treated mice and controls.

To further confirm whether the reduction in donor T cell activation after BMT was caused by the direct effect of R-Spo1 on T cells, we investigated the effect of R-Spo1 on T cells in vivo and in vitro. Administration of R-Spo1 over 3 d had no effect on the number of T cells in naive mice (Table I),

Table I. Brief administration of R-Spo1 had no effects on immunophenotype

Immunophenotype	+Control	+R-Spo1
Spleen		
$CD4^+$	20.7 ± 4.2	17.4 ± 2.0
$CD8^+$	14.3 ± 2.5	11.9 ± 0.9
$CD4^+Foxp3^+$	2.46 ± 0.63	2.46 ± 0.34
$B220^+$	58.5 ± 10.9	57.8 ± 2.9
Mesenteric lymph node		
$CD4^+$	4.3 ± 0.7	4.9 ± 0.2
$CD8^+$	3.5 ± 0.7	4.2 ± 0.4
$CD4^+Foxp3^+$	0.65 ± 0.14	0.70 ± 0.09
Thymus		
$CD4^+CD8^+$	96.2 ± 16.9	91.6 ± 19.8
$CD4^+$	8.4 ± 1.0	8.6 ± 2.1
$CD8^+$	3.4 ± 0.3	3.6 ± 0.6

B6 mice were intravenously injected with R-Spo1 (200 µg/day) or control for 3 d, and the spleen, mesenteric lymph nodes, and thymus were harvested 6 h later. Cell numbers are shown as mean ± SD ($\times 10^6$). Data are representative of two independent experiments ($n = 4$ for +control and +R-Spo1).

and the addition of R-Spo1 to culture did not affect in vitro T cell responses to alloantigens or anti-CD3 cross-linking (Fig. S2, A and B). Furthermore, R-Spo1 addition to culture affected neither the proliferation nor the generation of effector and memory $CD8^+$ and $CD4^+$ T cells in response to anti-CD3 cross-linking in vitro (Fig. S2, C–F).

Brief administration of R-Spo1 ameliorated systemic GVHD

We studied two lethal doses of TBI, 12 and 15 Gy, for their effects on GVHD. At both TBI doses, TCD controls showed 100% survival. All allogeneic controls receiving 15 Gy TBI died by day 40, whereas those receiving 12 Gy TBI displayed 7% survival at day 90 (Fig. 4 A). The TBI dose thus significantly correlated with GVHD mortality, as has been shown previously (Hill et al., 1997). In R-Spo1–treated animals, GVHD mortality was significantly reduced in experiments with 12 Gy TBI and delayed in those with 15 Gy TBI (Fig. 4 A) and reduced GVHD severity as assessed by clinical GVHD scores (Teshima et al., 2002a) in surviving animals (Fig. 4 B). Target organs, including the small intestine, liver, skin, and thymus, were then evaluated for signs of GVHD after allogeneic BMT after 12 Gy TBI. The small intestine and liver samples were harvested 1 wk after BMT, whereas skin and thymus samples were obtained 7 wk after BMT. GVHD-mediated thymic atrophy, characterized by a reduction in the numbers of $CD4^+CD8^+$ double-positive thymocytes, was significantly restored in R-Spo1–treated mice (Fig. 4 C). Pathological analysis of the small intestine, liver, and skin showed almost normal architecture in TCD controls (Fig. 4 D). In contrast, allogeneic controls showed severe blunting of villi and inflammatory infiltration, whereas R-Spo1–treated mice showed significant restoration of the small intestinal villous architecture with little inflammatory infiltration. Liver histology of allogeneic controls revealed mononuclear cell infiltration in bile ducts and portal triads (Fig. 4 D, arrowheads), whereas these changes were less prominent in R-Spo1–treated mice. Lesser lymphocyte infiltration was observed in the skin of R-Spo1–treated mice compared with that of allogeneic controls. GVHD pathology scores in each organ were significantly lower in R-Spo1–treated mice than those in controls (Fig. 4, E–G). Flow cytometric analysis of the spleens on day 35 displayed complete donor chimerism (99.9 ± 0.1%), ruling out mixed chimerism as a cause of the reduced GVHD. These results demonstrate that brief administration of R-Spo1 modulates not only intestinal but also systemic GVHD.

Next, we studied how the scheduling of R-Spo1 administration could influence the outcome of allogeneic BMT after 15 Gy TBI. Administration of R-Spo1 from day −3 to −1 and day 1–3 significantly prolonged survival. These beneficial effects were not observed when R-Spo1 was injected only once after BMT from day 1–6 after 15 Gy TBI (Fig. 4 H). When R-Spo1 was administered only once before TBI from day −6 to −1, early GVHD mortality was reduced; however, survival was not prolonged. These results suggest that R-Spo1 injection before TBI is mandatory and that posttransplant administration of R-Spo1 results in maximum reduction of GVHD.

Published January 31, 2011

R-Spo1 regulates GVHD by a mechanism dependent on repair of radiation-induced gut injury

To confirm that R-Spo1 ameliorated systemic GVHD by a mechanism dependent on repair of radiation-induced GI tract damage, the effects of R-Spo1 were evaluated in the same BMT model without conditioning, as previously described (Mori et al., 1998). Unirradiated B6D2F1 mice were intravenously injected with 12×10^7 splenocytes from MHC-mismatched B6 or B6-Ly5.1 donors on day 0. In this model, cytopenia mediated by donor T cell attack of BM is the primary cause of death in GVHD (Via et al., 1987). Injection of R-Spo1 did not impact the mortality or morbidity caused by GVHD (Fig. 5, A and B), donor T cell expansion (Fig. 5 C), thymic GVHD (Fig. 5 D), GVHD-associated cytopenia (Fig. 5 E), or donor cell engraftment (99.7 ± 0.4% in controls and 99.9 ± 0.0% in R-Spo1–treated mice on day 60).

DISCUSSION

Intestinal GVHD is characterized by severe villous atrophy and crypt degeneration. It has been suggested that crypt cell degeneration is one of the initial lesions of intestinal GVHD (Sale et al., 1979; Epstein et al., 1980; Mowat and Socie, 2004). ISCs reside in the intestinal crypts and play a pivotal role in both physiological tissue renewal and regeneration of the intestinal epithelium after injury. However, the identity of cells within the crypts (primary targets in GVHD) has been an

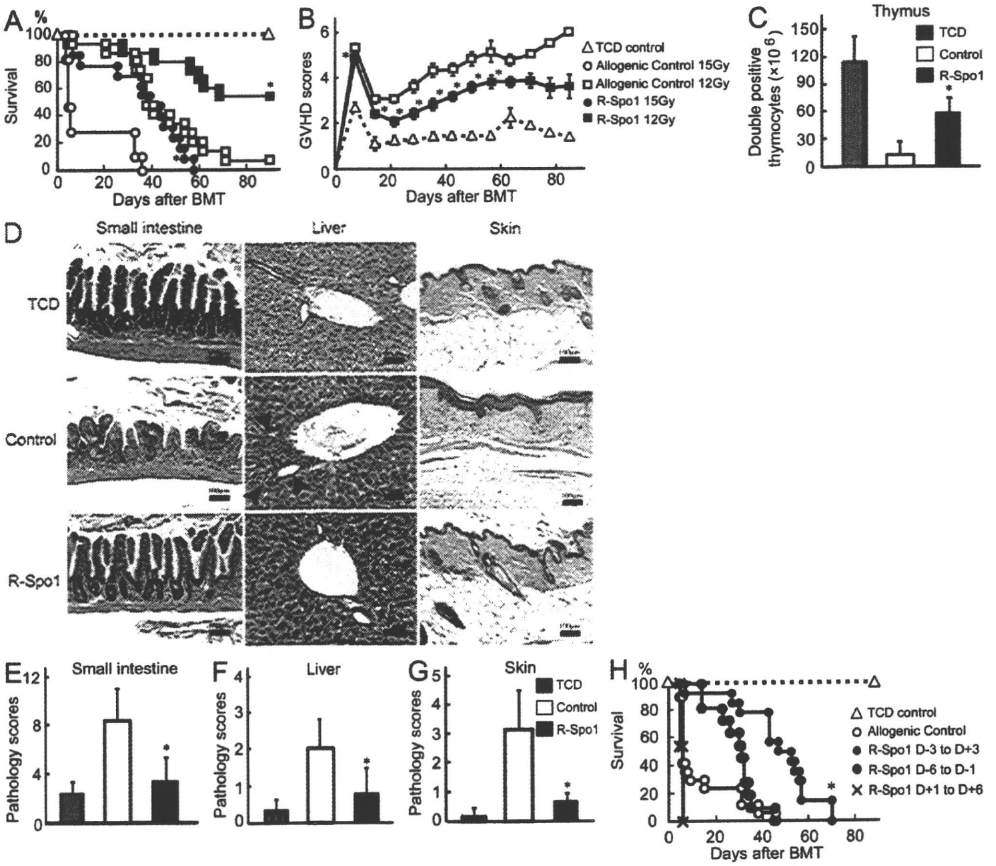

Figure 4. R-Spo1 modulated systemic GVHD. B6D2F1 mice were transplanted with 5×10^6 TCD BM cells with or without 2×10^6 T cells from B6 donors on day 0 after 15 or 12 Gy TBI. R-Spo1 (200 µg/day) or control was injected from day −3 to −1 and day 1–3 after BMT. (A and B) Survival (A) and clinical GVHD scores (B; means ± SE) are shown. TCD non-GVHD controls ($n = 6$), allogeneic controls with 15 Gy ($n = 11$) or 12 Gy TBI ($n = 15$), and R-Spo1 with 15 Gy ($n = 13$) or 12 Gy TBI ($n = 15$) are shown. Data from three independent experiments were combined. (C) Numbers of $CD4^+CD8^+$ double-positive thymocytes 7 wk after BMT (TCD, $n = 3$; control, $n = 5$; R-Spo1, $n = 5$). Data are representative of two similar experiments and are shown as means ± SD. (D) Representative histological findings of the small intestine, liver, and skin. Arrowheads indicate mononuclear cell infiltration in bile ducts and portal triads. Bars: (left and right) 100 µm; (middle) 50 µm. (E–G) Pathology scores of the small intestine (E) and liver (F) harvested on day 7 and those of the skin (G) harvested 7 wk after BMT after 12 Gy TBI (TCD, $n = 3$; control, $n = 5$; R-Spo1, $n = 5$). Data are representative of two similar experiments and are shown as means ± SD. (H) R-Spo1 was intravenously injected for six doses at different schedules after 15 Gy TBI and BMT. Survival after BMT: TCD non-GVHD controls ($n = 5$), allogeneic controls ($n = 17$), and R-Spo1 day −3 to −1 and day 1–3 (D-3 to D+3; $n = 11$), day −6 to −1 (D–6 to D–1; $n = 14$), or day 1–6 (D+1 to D+6; $n = 11$) are shown. Data from three independent experiments were combined. *, $P < 0.05$ compared with allogeneic controls.

Published January 31, 2011

enigma because of the lack of specific markers. In this study, we discovered that pretransplant TBI damaged *Olfm4*$^+$ ISCs in the crypts; however, the ISCs rapidly recovered and restored the normal architecture of the small intestine within 1 wk. With development of acute GVHD, the process of ISC recovery was inhibited, and prolonged and profound intestinal damage was induced after allogeneic BMT. These observations are well in line with those from a previous study of sequential rectal biopsies from patients undergoing allogeneic BMT (Epstein et al., 1980). Severe crypt degeneration was noted in all biopsies taken soon after BMT, probably because of the conditioning regimen. These changes persisted when acute GVHD was present but disappeared in patients who did not show clinical evidence of GVHD (Epstein et al., 1980). The current study thus affirms the long-held assumption that ISCs may be targets for immune responses associated with GVHD (Sale et al., 1979; Epstein et al., 1980; Mowat and Socie, 2004).

We have previously demonstrated that R-Spo1 induces rapid onset of epithelial proliferation in the intestine by stimulating Wnt signaling and protects against chemotherapy-induced colitis (Kim et al., 2005). However, owing to the lack of specific ISC markers it was unclear whether this effect was caused by the direct effect of R-Spo1 on ISCs. The current study shows that administration of R-Spo1 up-regulates the expression of Wnt target genes such as murine *Axin2*, *Ascl2*, and *Lgr5*. *Ascl2* is a critical transcriptional factor involved in controlling the fate of ISCs in adults (van der Flier et al., 2009b), and *Lgr5* marks ISCs (Barker et al., 2007, 2008). *Olfm4* is not a Wnt target gene but a highly specific and robust marker for *Lgr5*$^+$ ISCs (van der Flier et al., 2009a,b). We found that R-Spo1 stimulated proliferation of *Olfm4*$^+$ ISCs, thus taking further the observations from our previous study (Kim et al., 2005) and confirming recent observations that R-Spo1 enhances the proliferation of cycling ISCs via the Wnt signaling pathway (Bhanja et al., 2009; Sato et al., 2009).

Administration of R-Spo1 has been shown to mediate protection against radiation colitis, which is evident from studies in mouse models with chemotherapy- or radiation-induced mucositis and gut injury (Kim et al., 2005; Zhao et al., 2007, 2009; Bhanja et al., 2009). Our results suggest that R-Spo1–mediated protection of ISCs could be primarily responsible for the protection of the GI tract from radiation, as has been suggested in a recent study (Bhanja et al., 2009). Furthermore, we have shown that brief administration of R-Spo1 suppresses systemic GVHD after allogeneic BMT by a mechanism dependent on the repair of conditioning-induced GI tract injury. Experimental and clinical studies have suggested that GI tract damage resulting from both pretransplant conditioning regimens and GVHD plays a central role in increasing GVHD severity (Hill et al., 1997; Hill and Ferrara, 2000; Ferrara et al., 2003). Disruption of the GI mucosal barrier facilitates the translocation of immunostimulatory microbial products such as LPS into the systemic circulation (Hill et al., 1997; Cooke et al., 1998, 2001; Hill and Ferrara, 2000). LPS then stimulates mononuclear cells primed by donor T cell IFN-γ to produce large amounts of inflammatory cytokines such as TNF and IL-1 and augments donor T cell activation, thereby potentiating both inflammatory and cellular effectors of GVHD (Nestel et al., 1992; Cooke et al., 1998, 2001). The administration of R-Spo1 protected against GI tract damage, leading to the fortification of GI tract mucosal barrier functions and reduction of the subsequent inflammatory milieu. An inflammatory environment would have further enhanced donor T cell activation (Nestel et al., 1992; Hill et al., 1997; Cooke et al., 1998), and R-Spo1 treatment

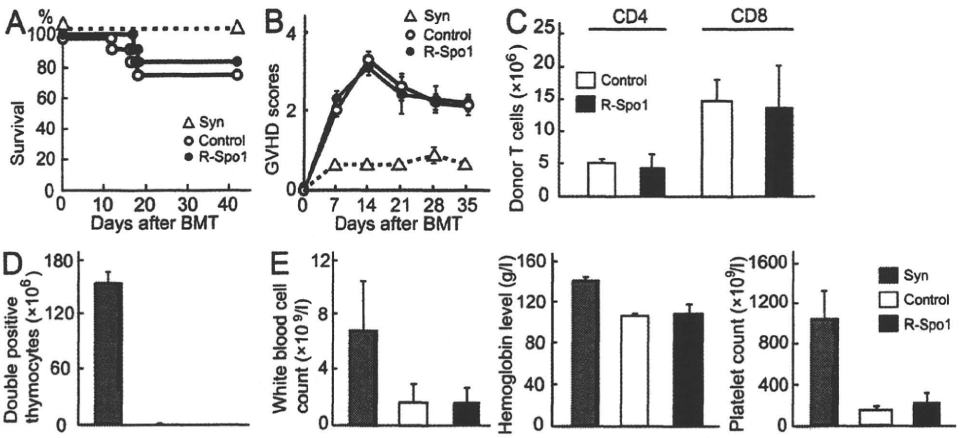

Figure 5. R-Spo1 failed to attenuate GVHD in unirradiated host. Unirradiated B6D2F1 mice were transplanted with 12 × 10^7 splenocytes from syngeneic or allogeneic B6 donors. R-Spo1 (200 µg/day) or control was administered from day −3 to −1 and day 1–3 after BMT. (A and B) Survival (A) and clinical GVHD scores (B; mean ± SE) are shown. Syngeneic controls (Syn; $n = 3$), allogeneic controls (control; $n = 12$), and R-Spo1 ($n = 12$) are shown. Data from two independent experiments were combined. (C–E) Numbers of donor CD4$^+$ and CD8$^+$ T cells in the spleen (C), CD4$^+$CD8$^+$ double-positive thymocytes (D), and a complete blood count (E) on day 14 (Syn, $n = 3$; control, $n = 4$; R-Spo1, $n = 4$) are shown. Data are representative of two independent experiments and are shown as mean ± SD.

Published January 31, 2011

was also found to significantly reduce donor T cell proliferation and activation. As a result, brief administration of R-Spo1 modulates not only intestinal GVHD but also systemic GVHD. This study thus demonstrates for the first time that ISC damage plays a critical role in the exaggeration of GVHD.

The protective effects of R-Spo1 were not observed after allogeneic BMT in the absence of a conditioning regimen, thus suggesting a mechanism dependent on repair of conditioning-induced GI tract injury. In addition, R-Spo1 may act through different mechanisms before and after TBI; it protects best against systemic GVHD when administered before and after transplantation. Treatment with R-Spo1 before TBI expanded ISCs, suggesting an increased number of surviving ISCs that play a pivotal role in the regeneration of intestinal epithelium after injury. Additional administration of R-Spo1 posttransplant may further enhance proliferation and differentiation of the surviving ISCs, thereby allowing the regeneration of intestinal epithelium and fortification of mucosal barrier functions to suppress subsequent inflammatory milieu. It has been shown that a single ISC is sufficient for the reconstitution of a crypt-villus unit (Sato et al., 2009).

Reduction in the activation of donor T cells after BMT did not appear to be caused by the direct effect of R-Spo1 on T cells. A recent study has shown that β-catenin–transduced $CD4^+CD25^+$ T reg cells survive longer than control cells, whereas β-catenin–transduced $CD4^+$ T cells become anergic (Ding et al., 2008). Wnt signaling arrests effector T cell differentiation by generating $CD8^+$ memory stem cells (Gattinoni et al., 2009). However, such changes were not apparent after BMT in our study. Wnt signaling is also important for hematopoiesis (Reya and Clevers, 2005); however, brief administration of R-Spo1 did not affect hematopoietic reconstitution after TCD BMT (unpublished data). We thus believe that R-Spo1 may preferentially stimulate ISCs rather than hematopoietic and T cells, as R-Spo1 transgenic mice show intestinal epithelial hyperplasia without any effects on lymphohematopoietic development (Kim et al., 2005). Alternately, such brief administration of R-Spo1 may not be sufficient to affect both the immune system and hematopoiesis. Wnt signaling has also been implicated in the pathogenesis of various tumors such as colon cancer and leukemia (Reya and Clevers, 2005; Román-Gómez et al., 2007). However, the incidence of tumorigenesis did not increase in R-Spo1 transgenic mice (Kim et al., 2006), and long-term treatment with R-Spo1 did not promote tumor xenograft growth in immunodeficient mice inoculated with various human colorectal tumor cell lines (Zhao et al., 2009). It thus follows that although caution should be exercised, it is unlikely that brief administration of R-Spo1 enhances tumorigenesis or the growth of preexisting tumors.

In summary, we found that ISCs are targets for GVHD and that protection of ISCs by R-Spo1 significantly improved the outcome of BMT by reducing systemic GVHD severity. By documenting that ISC damage is the key to this process, these results extend previous observations that the GI tract is not only a target organ for GVHD but also a crucial amplifier of systemic GVHD severity (Hill et al., 1998; Panoskaltsis-Mortari et al., 1998; Krijanovski et al., 1999; Teshima et al., 1999; Hill and Ferrara, 2000). An intensified conditioning regimen plays a critical role in controlling leukemia, but conditioning-related toxicity, particularly of the GI tract, limits the application of this curative therapy. Reduced intensity regimens have also been developed to explore the use of this therapy in older leukemic patients; however, better control of leukemia requires intensified conditioning in high-risk patients (Kahl et al., 2007). Thus, strategies to protect the GI tract from conditioning-related toxicity may allow safer application of intensified conditioning for controlling leukemia. Such a strategy has been tested in previous studies using IL-11 or keratinocyte growth factor. However, it is unfortunate that patients receiving IL-11 displayed severe fluid retention and early mortality (Antin et al., 2002), while keratinocyte growth factor failed to reduce conditioning regimen–mediated diarrhea (Blazar et al., 2006), thus making it impossible to further test the proposed strategy. R-Spo1 use is highly promising because of its direct, specific, and potent effects on ISCs; therefore, brief treatment with R-Spo1 may be used as an effective adjunct to clinical regimens of GVHD prophylaxis. This study presents a novel combined strategy for the rescue of both hematopoietic stem cells and ISCs in clinical medicine. Such a strategy may also be useful for treatment of other solid tumors and accidentally or intentionally irradiated victims, in whom damage to BM and the GI tract is a serious problem.

MATERIALS AND METHODS

Mice and reagents. Female B6 ($H\text{-}2^b$, $CD45.2^+$) and B6D2F1 ($H\text{-}2^{b/d}$, $CD45.2^+$) mice were purchased from Charles River, and B6-Ly5.1 ($H\text{-}2^b$, $CD45.1^+$) mice were obtained from the Jackson Laboratory. Mice were maintained as previously described (Teshima et al., 2002a). All animal experiments were performed under the auspices of the Institutional Animal Care and Research Advisory Committee. Recombinant human R-Spo1 was produced in CHO cells and purified as previously described (Zhao et al., 2007).

BMT. Mice were transplanted as previously described (Teshima et al., 2002a). In brief, after lethal TBI (x ray) delivered in two doses at 4-h intervals, B6D2F1 mice were intravenously injected with 5×10^6 TCD BM cells with or without 2×10^6 splenic T cells on day 0. Isolation of T cells and T cell depletion were performed using the T cell isolation kit and anti-CD90 microbeads, respectively, and AutoMACS (Miltenyi Biotec) according to the manufacturer's instructions. In some experiments, unirradiated B6D2F1 mice were intravenously injected with 12×10^7 splenocytes.

Assessment of GVHD. Survival after BMT was monitored daily, and the degree of clinical GVHD was assessed weekly by a scoring system that sums changes in five clinical parameters: weight loss, posture, activity, fur texture, and skin integrity (maximum index = 10) as described previously (Teshima et al., 2002a). Acute GVHD was also assessed by detailed histopathological analysis using a semiquantitative scoring system (Teshima et al., 2002a). Pictures from tissue sections were taken at room temperature using a digital camera (ProgRes 3012 mF; Jenoptik) mounted on a microscope (BX51; Olympus) and analyzed using a ProgRes PlugIn for PCI software version 5.0 (Jenoptik).

Flow cytometric analysis. mAbs used were FITC-, PE-, Cy5 PE-, or allophycocyanin-conjugated or biotinylated anti–mouse TCR-β, IFN-γ, CD4, CD8, CD25, CD45.1, CD45.2, CD44, CD62L, CD69, and B220 (BD),

Published January 31, 2011

and we also used Foxp3 (eBioscience). Surface marker staining and intracellular cytokine staining were performed as previously described (Teshima et al., 2002a; Asakura et al., 2010). At least 5,000 live samples were analyzed using FACSCalibur (BD) and FlowJo software (Tree Star, Inc.). The CFSE labeling of T cells was also performed as previously described (Teshima et al., 2002a).

Immunohistochemical staining and in situ hybridization. Slides were incubated at room temperature for 90 min with anti–mouse Ki-67 mAbs (Dako). We used Histofine Simple Stain MAXPO (rat) kits and subsequently diaminobenzidine solution (Nichirei) to generate brown-colored signals. Slides were then counterstained with hematoxylin. We measured villus height in 20 representative villi of the terminal ileum per slide as described previously (Farrell et al., 1998). For in situ hybridization, 1640-bp DNA fragments corresponding to nucleotide positions 17–435 of mouse *Olfm4* cDNA (GenBank/EMBL/DDBJ accession no. NM_001030294) were subcloned into pGEMT-Easy vectors (Promega) and used for generation of sense or antisense RNA probes. Digoxigenin-labeled RNA probes were prepared with DIG RNA labeling mix (Roche). Intestines were flushed, fixed in tissue fixative (Genostaff), embedded in paraffin, and sectioned at 6 µm. Sections were then dewaxed, rehydrated, and digested with proteinase K solution, refixed, treated in acetic anhydride solution, and hybridized for 16 h at 60°C with probes at concentrations of 100 ng/ml in probe diluent (Genostaff). After washing, the sections were treated with 0.5% blocking reagent (Roche) in TBST (TBS with Tween 20) for 30 min and then incubated with anti-digoxigenin alkaline phosphatase conjugate (Roche) diluted in a 1:1,000 ratio with TBST for 2 h. After washing, coloring reactions were performed with BM purple alkaline phosphatase substrate (Roche) overnight, and sections were then rewashed with PBS. Sections were then counterstained with Kernechtrot stain solution (Mutoh), dehydrated, and mounted with malinol (Mutoh).

Cell cultures. All culture media and incubation conditions have been previously described (Teshima et al., 2002b). Isolation of $CD8^+$ and $CD4^+CD25^-$ T cells was performed by AutoMACS according to the manufacturer's instructions. Methods to generate DCs were previously described (Teshima et al., 2002b). T cells were cultured at a concentration of 1×10^5 T cells/well with 2.5×10^3 irradiated DCs/well or with 5 µg/ml plate-bound anti-CD3 mAbs and 2 µg/ml anti-CD28 mAbs. Supernatants were collected for measurement of cytokine levels 96 h after the initiation of culture, and cell proliferation was determined by thymidine uptake assay.

ELISA. For measuring IFN-γ (BD) and TNF (R&D systems) levels, we performed ELISA according to the manufacturers' instructions with sensitivities of 31.25 pg/ml and 23.4 pg/ml, respectively. The Limulus amebocyte lysate assay (Lonza) was performed according to the manufacturer's instructions to determine the serum level of LPS with a sensitivity of 0.1 EU/ml. All units expressed are relative to the US reference standard EC-2.

Quantitative real-time PCR analysis. Total RNA was purified using the RNeasy kit (QIAGEN). cDNA was synthesized using a QuantiTect reverse transcription kit (QIAGEN). PCR reactions and analyses were performed with ABI PRISM 7900HT SDS 2.1 (Applied Biosystems) using TaqMan Universal PCR master mix (Applied Biosystems), primers, and labeled TaqMan probes (TaqMan Gene Expression Assays; Applied Biosystems). The relative amount of each messenger RNA was determined using the standard curve method and was normalized to the level of GAPDH in each sample.

Statistical analysis. Mann-Whitney *U* tests were used to compare data, the Kaplan-Meier product limit method was used to obtain survival probability, and the log-rank test was applied to compare survival curves. $P < 0.05$ was considered statistically significant.

Online supplemental material. Fig. S1 demonstrates that R-Spo1 stimulated proliferation of ISCs through the Wnt signaling pathway. Fig. S2 shows that R-Spo1 has no effects on proliferation and effector differentiation of T cells in response to CD3 or alloantigen stimulation in vitro. Online supplemental material is available at http://www.jem.org/cgi/content/full/jem.20101559/DC1.

This study was supported by research funds from the Ministry of Education, Culture, Sports, Science and Technology (no. 20659153 to T. Teshima), Health and Labor Science Research Grants (to T. Teshima), and a grant from the Foundation for Promotion of Cancer Research (Tokyo, Japan to T. Teshima).

The authors have no conflicting financial interests.

Submitted: 2 August 2010
Accepted: 12 January 2011

REFERENCES

Antin, J.H., S.J. Lee, D. Neuberg, E. Alyea, R.J. Soiffer, S. Sonis, and J.L. Ferrara. 2002. A phase I/II double-blind, placebo-controlled study of recombinant human interleukin-11 for mucositis and acute GVHD prevention in allogeneic stem cell transplantation. *Bone Marrow Transplant.* 29:373–377. doi:10.1038/sj.bmt.1703394

Asakura, S., D. Hashimoto, S. Takashima, H. Sugiyama, Y. Maeda, K. Akashi, M. Tanimoto, and T. Teshima. 2010. Alloantigen expression on non-hematopoietic cells reduces graft-versus-leukemia effects in mice. *J. Clin. Invest.* 120:2370–2378. doi:10.1172/JCI39165

Barker, N., J.H. van Es, J. Kuipers, P. Kujala, M. van den Born, M. Cozijnsen, A. Haegebarth, J. Korving, H. Begthel, P.J. Peters, and H. Clevers. 2007. Identification of stem cells in small intestine and colon by marker gene Lgr5. *Nature.* 449:1003–1007. doi:10.1038/nature06196

Barker, N., M. van de Wetering, and H. Clevers. 2008. The intestinal stem cell. *Genes Dev.* 22:1856–1864. doi:10.1101/gad.1674008

Batlle, E., J.T. Henderson, H. Beghtel, M.M. van den Born, E. Sancho, G. Huls, J. Meeldijk, J. Robertson, M. van de Wetering, T. Pawson, and H. Clevers. 2002. Beta-catenin and TCF mediate cell positioning in the intestinal epithelium by controlling the expression of EphB/ephrinB. *Cell.* 111:251–263. doi:10.1016/S0092-8674(02)01015-2

Bhanja, P., S. Saha, R. Kabarriti, L. Liu, N. Roy-Chowdhury, J. Roy-Chowdhury, R.S. Sellers, A.A. Alfieri, and C. Guha. 2009. Protective role of R-spondin1, an intestinal stem cell growth factor, against radiation-induced gastrointestinal syndrome in mice. *PLoS One.* 4:e8014. doi:10.1371/journal.pone.0008014

Binnerts, M.E., K.A. Kim, J.M. Bright, S.M. Patel, K. Tran, M. Zhou, J.M. Leung, Y. Liu, W.E. Lomas III, M. Dixon, et al. 2007. R-Spondin1 regulates Wnt signaling by inhibiting internalization of LRP6. *Proc. Natl. Acad. Sci. USA.* 104:14700–14705. doi:10.1073/pnas.0702305104

Blazar, B.R., D.J. Weisdorf, T. Defor, A. Goldman, T. Braun, S. Silver, and J.L. Ferrara. 2006. Phase 1/2 randomized, placebo-control trial of palifermin to prevent graft-versus-host disease (GVHD) after allogeneic hematopoietic stem cell transplantation (HSCT). *Blood.* 108:3216–3222. doi:10.1182/blood-2006-04-017780

Cooke, K.R., G.R. Hill, J.M. Crawford, D. Bungard, Y.S. Brinson, J. Delmonte Jr., and J.L. Ferrara. 1998. Tumor necrosis factor- alpha production to lipopolysaccharide stimulation by donor cells predicts the severity of experimental acute graft-versus-host disease. *J. Clin. Invest.* 102:1882–1891. doi:10.1172/JCI4285

Cooke, K.R., A. Gerbitz, J.M. Crawford, T. Teshima, G.R. Hill, A. Tesolin, D.P. Rossignol, and J.L. Ferrara. 2001. LPS antagonism reduces graft-versus-host disease and preserves graft-versus-leukemia activity after experimental bone marrow transplantation. *J. Clin. Invest.* 107:1581–1589. doi:10.1172/JCI12156

Ding, Y., S. Shen, A.C. Lino, M.A. Curotto de Lafaille, and J.J. Lafaille. 2008. Beta-catenin stabilization extends regulatory T cell survival and induces anergy in nonregulatory T cells. *Nat. Med.* 14:162–169. doi:10.1038/nm1707

Epstein, R.J., G.B. McDonald, G.E. Sale, H.M. Shulman, and E.D. Thomas. 1980. The diagnostic accuracy of the rectal biopsy in acute graft-versus-host disease: a prospective study of thirteen patients. *Gastroenterology.* 78:764–771.

Farrell, C.L., J.V. Bready, K.L. Rex, J.N. Chen, C.R. DiPalma, K.L. Whitcomb, S. Yin, D.C. Hill, B. Wiemann, C.O. Starnes, et al. 1998. Keratinocyte growth factor protects mice from chemotherapy and radiation-induced gastrointestinal injury and mortality. *Cancer Res.* 58:933–939.

Ferrara, J.L., K.R. Cooke, and T. Teshima. 2003. The pathophysiology of acute graft-versus-host disease. *Int. J. Hematol.* 78:181–187. doi:10.1007/BF02983793

Gattinoni, L., X.S. Zhong, D.C. Palmer, Y. Ji, C.S. Hinrichs, Z. Yu, C. Wrzesinski, A. Boni, L. Cassard, L.M. Garvin, et al. 2009. Wnt signaling arrests effector T cell differentiation and generates CD8+ memory stem cells. *Nat. Med.* 15:808–813. doi:10.1038/nm.1982

Hill, G.R., and J.L. Ferrara. 2000. The primacy of the gastrointestinal tract as a target organ of acute graft-versus-host disease: rationale for the use of cytokine shields in allogeneic bone marrow transplantation. *Blood.* 95:2754–2759.

Hill, G.R., J.M. Crawford, K.R. Cooke, Y.S. Brinson, L. Pan, and J.L. Ferrara. 1997. Total body irradiation and acute graft-versus-host disease: the role of gastrointestinal damage and inflammatory cytokines. *Blood.* 90:3204–3213.

Hill, G.R., K.R. Cooke, T. Teshima, J.M. Crawford, J.C. Keith Jr., Y.S. Brinson, D. Bungard, and J.L. Ferrara. 1998. Interleukin-11 promotes T cell polarization and prevents acute graft-versus-host disease after allogeneic bone marrow transplantation. *J. Clin. Invest.* 102:115–123. doi:10.1172/JCI3132

Kahl, C., B.E. Storer, B.M. Sandmaier, M. Mielcarek, M.B. Maris, K.G. Blume, D. Niederwieser, T.R. Chauncey, S.J. Forman, E. Agura, et al. 2007. Relapse risk in patients with malignant diseases given allogeneic hematopoietic cell transplantation after nonmyeloablative conditioning. *Blood.* 110:2744–2748. doi:10.1182/blood-2007-03-078592

Kim, K.A., M. Kakitani, J. Zhao, T. Oshima, T. Tang, M. Binnerts, Y. Liu, B. Boyle, E. Park, P. Emtage, et al. 2005. Mitogenic influence of human R-spondin1 on the intestinal epithelium. *Science.* 309:1256–1259. doi:10.1126/science.1112521

Kim, K.A., J. Zhao, S. Andarmani, M. Kakitani, T. Oshima, M.E. Binnerts, A. Abo, K. Tomizuka, and W.D. Funk. 2006. R-Spondin proteins: a novel link to beta-catenin activation. *Cell Cycle.* 5:23–26. doi:10.4161/cc.5.1.2305

Krijanovski, O.I., G.R. Hill, K.R. Cooke, T. Teshima, J.M. Crawford, Y.S. Brinson, and J.L. Ferrara. 1999. Keratinocyte growth factor separates graft-versus-leukemia effects from graft-versus-host disease. *Blood.* 94:825–831.

Mori, T., T. Nishimura, Y. Ikeda, T. Hotta, H. Yagita, and K. Ando. 1998. Involvement of Fas-mediated apoptosis in the hematopoietic progenitor cells of graft-versus-host reaction-associated myelosuppression. *Blood.* 92:101–107.

Mowat, M., and G. Socie. 2004. Intestinal Graft-vs.-Host Disease. *In* Graft-vs.-Host Disease. Third edition. J.L. Ferrara, K.R. Cooke, and H.J. Deeg, editors. Marcel Dekker, New York. 279–327.

Nestel, F.P., K.S. Price, T.A. Seemayer, and W.S. Lapp. 1992. Macrophage priming and lipopolysaccharide-triggered release of tumor necrosis factor alpha during graft-versus-host disease. *J. Exp. Med.* 175:405–413. doi:10.1084/jem.175.2.405

Panoskaltsis-Mortari, A., D.L. Lacey, D.A. Vallera, and B.R. Blazar. 1998. Keratinocyte growth factor administered before conditioning ameliorates graft-versus-host disease after allogeneic bone marrow transplantation in mice. *Blood.* 92:3960–3967.

Pinto, D., A. Gregorieff, H. Begthel, and H. Clevers. 2003. Canonical Wnt signals are essential for homeostasis of the intestinal epithelium. *Genes Dev.* 17:1709–1713. doi:10.1101/gad.267103

Reya, T., and H. Clevers. 2005. Wnt signalling in stem cells and cancer. *Nature.* 434:843–850. doi:10.1038/nature03319

Román-Gómez, J., L. Cordeu, X. Agirre, A. Jiménez-Velasco, E. San José-Eneriz, L. Garate, M.J. Calasanz, A. Heiniger, A. Torres, and F. Prosper. 2007. Epigenetic regulation of Wnt-signaling pathway in acute lymphoblastic leukemia. *Blood.* 109:3462–3469. doi:10.1182/blood-2006-09-047043

Sale, G.E., H.M. Shulman, G.B. McDonald, and E.D. Thomas. 1979. Gastrointestinal graft-versus-host disease in man. A clinicopathologic study of the rectal biopsy. *Am. J. Surg. Pathol.* 3:291–299. doi:10.1097/00000478-197908000-00001

Sato, T., R.G. Vries, H.J. Snippert, M. van de Wetering, N. Barker, D.E. Stange, J.H. van Es, A. Abo, P. Kujala, P.J. Peters, and H. Clevers. 2009. Single Lgr5 stem cells build crypt-villus structures in vitro without a mesenchymal niche. *Nature.* 459:262–265. doi:10.1038/nature07935

Teshima, T., G.R. Hill, L. Pan, Y.S. Brinson, M.R. van den Brink, K.R. Cooke, and J.L. Ferrara. 1999. IL-11 separates graft-versus-leukemia effects from graft-versus-host disease after bone marrow transplantation. *J. Clin. Invest.* 104:317–325. doi:10.1172/JCI7111

Teshima, T., R. Ordemann, P. Reddy, S. Gagin, C. Liu, K.R. Cooke, and J.L. Ferrara. 2002a. Acute graft-versus-host disease does not require alloantigen expression on host epithelium. *Nat. Med.* 8:575–581. doi:10.1038/nm0602-575

Teshima, T., P. Reddy, K.P. Lowler, M.A. KuKuruga, C. Liu, K.R. Cooke, and J.L. Ferrara. 2002b. Flt3 ligand therapy for recipients of allogeneic bone marrow transplants expands host CD8 alpha(+) dendritic cells and reduces experimental acute graft-versus-host disease. *Blood.* 99:1825–1832. doi:10.1182/blood.V99.5.1825

van der Flier, L.G., A. Haegebarth, D.E. Stange, M. van de Wetering, and H. Clevers. 2009a. OLFM4 is a robust marker for stem cells in human intestine and marks a subset of colorectal cancer cells. *Gastroenterology.* 137:15–17. doi:10.1053/j.gastro.2009.05.035

van der Flier, L.G., M.E. van Gijn, P. Hatzis, P. Kujala, A. Haegebarth, D.E. Stange, H. Begthel, M. van den Born, V. Guryev, I. Oving, et al. 2009b. Transcription factor achaete scute-like 2 controls intestinal stem cell fate. *Cell.* 136:903–912. doi:10.1016/j.cell.2009.01.031

Via, C.S., S.O. Sharrow, and G.M. Shearer. 1987. Role of cytotoxic T lymphocytes in the prevention of lupus-like disease occurring in a murine model of graft-vs-host disease. *J. Immunol.* 139:1840–1849.

Zhao, J., J. de Vera, S. Narushima, E.X. Beck, S. Palencia, P. Shinkawa, K.A. Kim, Y. Liu, M.D. Levy, D.J. Berg, et al. 2007. R-spondin1, a novel intestinotrophic mitogen, ameliorates experimental colitis in mice. *Gastroenterology.* 132:1331–1343. doi:10.1053/j.gastro.2007.02.001

Zhao, J., K.A. Kim, J. De Vera, S. Palencia, M. Wagle, and A. Abo. 2009. R-Spondin1 protects mice from chemotherapy or radiation-induced oral mucositis through the canonical Wnt/beta-catenin pathway. *Proc. Natl. Acad. Sci. USA.* 106:2331–2336. doi:10.1073/pnas.0805159106

RHEUMATOLOGY

Rheumatology 2011;50:944–952
doi:10.1093/rheumatology/keq414
Advance Access publication 20 December 2010

Original article

Analysis of immune reconstitution after autologous CD34$^+$ stem/progenitor cell transplantation for systemic sclerosis: predominant reconstitution of Th1 CD4$^+$ T cells

Hiroshi Tsukamoto[1], Koji Nagafuji[1], Takahiko Horiuchi[1], Hiroki Mitoma[1], Hiroaki Niiro[1], Yojiro Arinobu[2], Yasushi Inoue[1], Kentaro To[1], Toshihiro Miyamoto[1], Hiromi Iwasaki[2], Takanori Teshima[2], Mine Harada[1,3] and Koichi Akashi[1]

Abstract

Objective. The aim of this study is to evaluate the mechanism of long-term effect of autologous haematopoietic stem cell transplantation (ASCT) in treatment of SSc.

Methods. Eleven patients (three males and eight females) with SSc were enrolled. Blood mononuclear cells were harvested after mobilization treatment with CYC and G-CSF. CD34$^+$ haematopoietic stem/progenitor cell fractions were purified and cryopreserved. Patients were transplanted with $>2 \times 10^6$/kg autologous CD34$^+$ cells after high-dose CYC (50 mg/kg for 4 days) conditioning. Immune reconstitution was evaluated serially by analysing lymphocyte subpopulations for 36 months.

Results. Progressive improvement of skin sclerosis has been observed for 3 years in most of the patients. The serum level of anti-Scl-70, an auto-antibody specific to SSc, was progressively decreased after ASCT. Improvement of skin sclerosis was significantly associated with the change in the serum anti-Scl-70 level after ASCT at 36 months. Serum levels of KL-6 and surfactant protein D, indicators for interstitial pneumonia activity, were also significantly decreased. The number of CD8$^+$ T cells immediately recovered within a month after ASCT, while the number of CD4$^+$ T cells remained low for >36 months post-transplant. The majority of CD4$^+$ cells were memory but not naïve T cells, and regulatory CD4$^+$ T cells were not recovered. Th1/Th2 ratio was significantly increased after ASCT.

Conclusions. ASCT with purified CD34$^+$ cells was effective in controlling the disease activity of SSc. Th1/Th2 ratio was significantly increased for at least 3 years after ASCT.

Key words: Autoimmune disease, High-dose cyclophosphamide, Transplantation, Immune reconstitution, Th1/Th2 balance.

CLINICAL SCIENCE

Introduction

SSc is a heterogeneous autoimmune disease (AD) characterized by predominant T-cell activation, production of auto-antibodies and cytokine release [1, 2]. All of these contribute to diffuse microvascular injury, leading to diffuse sclerosis within the skin and internal organs. DcSSc and internal organ involvement often cause life-threatening status of patients [3].

Autologous haematopoietic stem cell transplantation (ASCT) was introduced for SSc treatment in 1996, and >100 patients with SSc have been treated [4]. Phase I–II studies demonstrated that improvement of skin sclerosis and stabilization of interstitial pneumonia (IP) were achieved [5–10]. We also reported the safety and efficacy of high-dose CYC with ASCT for SSc patients [11]. The complete or partial remission of SSc was maintained for at least 3 years in these reports [6–9].

[1]Department of Medicine and Biosystemic Science, Kyushu University Graduate School of Medical Sciences, Maidashi, Higashi-ku, [2]Center for Cellular and Molecular Medicine, Kyushu University Hospital, Fukuoka and [3]National Hospital Organization, Omuta Hospital, Omuta, Japan.

Submitted 22 January 2010; revised version accepted 16 November 2010.

Correspondence to: Hiroshi Tsukamoto, Department of Medicine and Biosystemic Science, Kyushu University Graduate School of Medical Sciences, 3-1-1 Maidashi, Higashi-ku, Fukuoka 812-8582, Japan. E-mail: tsukamot@intmed1.med.kyushu-u.ac.jp

The working hypotheses of the efficacy of ASCT for SSc might be due to the immune reset that should include: (i) the eradication of auto-reactive lymphocytes by immunoablative conditioning; and/or (ii) the correction of dysregulated immune balance by newly developed lymphocytes derived from transplanted haematopoietic stem cells [12]. However, there remains controversy regarding whether such immune reset occurs in patients treated with ASCT. Muraro *et al.* [13] have reported that naïve CD4+ T cells with diverse T-cell receptor repertoire, which were generated through thymus, developed after ASCT in patients with multiple sclerosis (MS). In contrast, in SSc patients, Farge *et al.* [14] reported the sustained reduction of CD4+ T cells and B cells after ASCT.

Furthermore, Th1/Th2 balance might also be important in understanding the disease status of SSc. In a tight skin mouse, an animal model for SSc, the stimulation of Th1 immune responses prevents the development of scleroderma-like syndrome [15]. In human SSc, a shift from Th2 to Th1 responses is correlated with improvement of the skin fibrosis by longitudinal analysis of serum cytokine concentrations [16].

These data led us to analyse immune reconstitution in SSc patients treated with ASCT. In this study, we tracked reconstitution of T- and B-cell subpopulations after ASCT with purified CD34+ haematopoietic stem/progenitor cells in SSc patients, and found that despite the resolution of clinical symptoms of SSc, patients did not achieve normalization of lymphocyte compartment, even 3 years after ASCT. All patients showed sustained reduction of CD4 T cells, but Th1/Th2 ratio was increased during the 3-year observation. Thus, the clinical efficacy of ASCT might be dependent upon the skewed reconstitution of Th1 cells for a long time after ASCT.

Patients and methods

The study was approved by the ethics committee of Kyushu University Hospital. Written informed consent was obtained from all patients according to the Declaration of Helsinki.

Patients and eligibility

Eligibility of patients with SSc for ASCT was previously described [11]. Briefly, patients with SSc were eligible when they had severe diffuse SSc that had rapidly developed over the previous 4 years. They also had to have at least one of the following organ involvements: (i) pulmonary, (ii) cardiac or (iii) renal involvement. Patients with limited SSc were considered eligible when progressive and life-threatening IP was present. Patients were excluded from the study when they had uncontrolled arrhythmia, severe heart failure, pulmonary hypertension, DL_{CO} <20% of predicted and renal failure as previously described [11]. All patients were followed up for at least 36 months after transplantation for the evaluation of immune reconstitution. Blood was obtained from healthy donors (after informed consent, $n = 10$) to determine the reference values of lymphocyte subpopulations and Th1/Th2 balance, and from SSc patients (after informed consent, $n = 13$) for FoxP3 staining.

Peripheral blood stem cell collection and ASCT

Peripheral blood stem cells (PBSCs) were mobilized during haematologic recovery after relatively high-dose CYC (2 g/m^2) for 2 days followed by administration of recombinant human G-CSF (filgrastim; Kirin Brewery, Tokyo, Japan) as previously described [11]. After collecting PBSCs to obtain 2×10^6 CD34+cells/kg or more by apheresis, CD34+ cells were positively selected using an immunomagnetic bead with an anti-CD34 mAb (CliniMACS; Miltenyi Biotec, Germany). For pre-transplant conditioning, high-dose CYC (50 mg/kg) was given for 4 days from Day -5 to -2 and frozen-thawed CD34+ cells were transplanted on Day 0. Patients 1, 2, 3, 4 and 6 received G-CSF from Day 1 [11]. Concomitantly administered prednisolone doses were kept unchanged or gradually tapered according to the individual clinical status after ASCT. The concomitantly administered immunosuppressants were stopped before the administration of CYC for mobilization.

Treatment outcome

The modified Rodnan skin score (mRSS) was used to evaluate the improvement of skin sclerosis when initial mRSS was ⩾15 [11]. Serum levels of anti-Scl 70 (anti-topo I) antibody were measured by an ELISA kit (MBL, Nagoya, Japan). Serum levels of KL-6 and surfactant protein D (SP-D) were measured by ELISA kits (Sanko Junyaku Co., Tokyo and Yamasa Co., Choshi, respectively, Japan). Serum levels of immunoglobulin were measured by laser nephelometry.

Lymphocyte phenotyping

Lymphocyte immunophenotyping of samples from whole blood was performed by IF flow cytometry before mobilization, before haematopoietic stem cell transplantation (HSCT) and 1, 3, 6, 12, 18, 24, 36 months after HSCT. The following mAbs and their combinations were used: anti-CD3-FITC; anti-CD19-phycoerythrin (PE); anti-CD20-FITC; anti-CD4-FITC; anti-CD8-PE; anti-CD45RA-PE; anti-CD45RO-PE; anti-CD25-PE; anti-CD16-FITC; anti-CD56-PE, anti-CD69-FITC and anti-CD27-FITC (eBioscience, San Diego, CA, USA). The CD4+FoxP3+ cells were detected by using anti-CD4-FITC, anti-FoxP3-PE and permeabilization buffer (eBioscience) in 9 patients at 37.8 (18.0) months (one sample for each patient) after ASCT and 13 SSc controls without ASCT. Results were expressed as the absolute number of cells.

Th1/Th2 balance

Flow cytometric determination of IFN-γ and IL-4 in the cytoplasm of peripheral CD4+ T cells was performed by a previously described method [17]. Briefly, aliquots (500 μl) of heparinized whole blood were stimulated with a combination of 25 ng/ml phorbol myristate acetate (PMA) and 1 μg/ml ionomycin in the presence of brefeldin A (Sigma, St Louis, MO, USA) and cultured for 4 h at 37°C

in a humidified incubator containing 7% CO_2. Activated cultures were aliquoted and stained with 20 μl of peridinin chlorophyll protein-conjugated CD4-specific mAb (Becton Dickinson, San Jose, CA, USA) for 15 min at room temperature, and then treated with 2 ml of FACS lysing solution (Becton Dickinson). After a short incubation (5 min), the samples were centrifuged and combined with FACS permeabilizing solution (Becton Dickinson) for 10 min at room temperature in the dark. The sample tubes were washed twice and FITC-conjugated IFN-γ-specific mAb and PE-conjugated IL-4-specific mAb (Becton Dickinson) for 30 min at room temperature in the dark. FITC-conjugated mouse IgG2a and PE-conjugated mouse IgG1 were used as controls. After washing again, the cells were resuspended in 1% paraformaldehyde and analysed by flow cytometry. The percentage of IFN-γ or IL-4-positive cells (percentage of IFN-γ or percentage of IL-4) was counted by FACS, and Th1/Th2 balance was evaluated by a ratio of percentage of IFN-γ to percentage of IL-4 (IFN-γ/IL-4).

Cytokine and chemokine levels

Serum levels of TNF-α and TGF-β were measured with sandwich ELISA kits (Quantikine; R&D systems, Minneapolis, MN, USA), according to the manufacturer's instructions before and after ASCT. Serum levels of IL-6 and soluble receptor for IL-2 (sIL-2R) were measured with CLISA kit (Fujirebio, Tokyo, Japan) and with ELISA kit (Kyowamedix, Tokyo, Japan), respectively.

Statistical analysis

Values were expressed as mean (S.D.). Student's *t*-test was used for statistical analysis of the data. The correlations of mRSS with the level of anti-Scl-70 or Th1/Th2 balance were investigated by Pearson's correlation coefficient test. Difference with $P < 0.05$ was considered to be statistically significant.

Results

Autologous transplantation with purified CD34$^+$ mobilized blood stem cells was successfully performed without treatment-related mortality

Eleven patients, eight females and three males, were enrolled in this study. Clinical results of Patients 1-6 at 12 months after ASCT were previously reported [11]. The mean (S.D.) of mRSS was 21.5 (9.0), and all patients developed clinical IP with decreased per cent vital capacity (VC) and per cent DL_{CO} [mean (S.D.), 64.9 (14.8) and 45.8 (18.0)%, respectively] (Table 1). The anti-Scl-70 antibody, an auto-antibody specific to diffuse SSc, was detected in 9 out of 11 patients. All patients were resistant to the standard treatment with CS, CYC and/or ciclosporin. Blood mononuclear cells were harvested after mobilization with CYC and G-CSF. CD34$^+$ haematopoietic stem/progenitor cell fractions were purified and cryopreserved. Patients were transplanted with purified autologous CD34$^+$ cells after high-dose CYC (500 mg/kg) conditioning. Consequentially, 4.7×10^6/kg CD34$^+$ cells with 1.1 (1.2) $\times 10^4$/kg CD3$^+$ T-cell contaminants were transplanted. ASCT was successfully performed without transplantation-related mortality in all patients, but Patient 7 died due to the progression of IP at 20 months after ASCT. The clinical status of the remaining 10 patients was followed up for >36 months. There was a variety of post-transplant infections such as adenoviral haemorrhagic cystitis, herpes zoster and cytomegaloviral antigenaemia [18].

CD34$^+$ ASCT treatment induced resolution of refractory SSc

The effect of ASCT on skin sclerosis was assessed by the change in mRSS. After ASCT, skin sclerosis was progressively resolved, and had improved by 72.0% at 36 months post-transplant (Fig. 1A). The vital capacity of the lung was increased from 64.9 to 77.8% at 36 months, although

Table 1 Patient profile and number of reinfused cells

Patient number	Sex	Age, years	mRSS	IP	%VC/DL_{Co}	Anti-Scl-70	Prior therapy	Follow-up, month	Number of reinfused CD34$^+$ cells ($\times 10^6$/kg)	Number of reinfused CD3$^+$ cells ($\times 10^4$/kg)
1	F	54	16	+	58/51	+	St, CYC	88	8.4	0.33
2	M	55	15	+	65/47	+	St	78	4.9	0.27
3	M	58	31	+	63/44	–	St	77	2.2	2.95
4	F	54	26	+	73/60	+	St	75	2.1	1.71
5	F	53	28	+	74/29	+	St	72	7.2	3.0
6	F	48	32	+	77/25	+	St, CYC, CsA	68	4.0	2.35
7	F	34	8	+	39/ND	–	-	20	9.1	1.03
8	F	61	26	+	90/87	+	St	52	3.0	0.32
9	F	61	32	+	56/37	+	St, CsA	47	4.2	0.13
10	F	44	15	+	45/35	+	St, CY	43	4.9	0.0
11	M	53	7	+	74/44	+	St	39	1.3	0.26
Ave. (S.D.)		52.3 (7.5)	21.5 (9.0)		64.9 (14.8)/45.8 (18.0)			60.0 (21.0)	4.7 (2.6)	1.1 (1.2)

F: female; M: male; Ave.: Average; ND: not done.

DL_{CO} was unchanged (Fig. 1B). Serum levels of KL-6 and SP-D, indicators of IP activity [19, 20], were significantly decreased (Fig. 1C and D).

Reflecting the resolution of clinical symptoms of SSc, the serum level of anti-Scl-70 progressively decreased after ASCT (Fig. 2A), independent of serum immunoglobulin levels (Fig. 2B). A significant correlation ($r = 0.52$, $P < 0.05$) was observed between the change in mRSS and that in the serum level of anti-Scl-70 at 36 months after ASCT.

Serum levels of pro-inflammatory or pro-fibrotic cytokines and a T-cell activation marker such as TNF-α, TGF-β, IL-6 and soluble IL-2R (sIL-2R), were also decreased after ASCT (Fig. 3A–D). These data show that ASCT with purified $CD34^+$ cells is effective in controlling disease activity of SSc patients refractory to conventional immunosuppressive therapies.

The recovery of $CD4^+$ T cells was particularly retarded after ASCT with purified $CD34^+$ cells in SSc patients

Because the patients were infused with highly purified $CD34^+$ haematopoietic stem/progenitor cells containing very low numbers of lymphocytes, we tracked the immune reconstitution after ASCT by analysing lymphocyte subpopulations for 36 months.

As shown in Fig. 4A, although the absolute number of $CD8^+$ T cells returned to the normal level only a month after ASCT, the recovery of $CD4^+$ T cells was apparently retarded; at 36 months post-transplant, the number of $CD4^+$ cells remained below the normal range, resulting in continuous inversion of the CD4/CD8 ratio. Previous reports have shown that the long-term remission after ASCT in MS and SLE was associated with the increased number of thymus-derived naïve $CD4^+$ T cells [13, 21]. Therefore, we analysed functional subsets of $CD4^+$ T cells. As shown in Fig. 4B, the number of memory $CD4^+CD45RO^+$ T cells was significantly decreased for 1–3 months after $CD34^+$ ASCT, but returned to the baseline level 24 months after ASCT, although it did not reach the normal range. In contrast, naïve $CD4^+CD45RA^+$ T cells were significantly decreased after mobilization, and remained at a low level at 36 months post-ASCT. These data show that most recovered $CD4^+$ T cells were memory cells but not naïve T cells. The $CD4^+CD25^+$ T cell fraction that includes activated and regulatory T cells [22] disappeared after ASCT, and remained low in number even at 36 months post-ASCT (Fig. 4C). The number of $CD4^+FoxP3^+$ cells in 9 patients at 37.8 (18.0) months after ASCT was significantly lower than that of 13 SSc controls [8.06 (7.61) *vs* 27.23 (13.30)/μl, $P < 0.05$]. These results show that although the patients displayed resolution of clinical SSc after ASCT, naïve $CD45RA^+$ T cells or regulatory T cells did not reconstitute well after ASCT.

SSc patients have distinct abnormalities of B-cell subpopulations, characterized by expanded naïve B cells and activated but diminished memory B cells [23]. The number of $CD19^+$ B cells returned into the normal range 18 months after ASCT.

Fig. 1 Resolution of SSc after ASCT. (**A**) mRSS. The proportional change from baseline measurement was calculated for each time point. Patients with an initial mRSS of ⩾15 were included. (**B**) VC and DL_{CO}. (**C**) KL-6. (**D**) SP-D. Data are presented as mean (S.D.). The *x*-axis is not drawn to scale. The data obtained before mobilization and just before transplantation (HSCT) are shown as BM and BT, respectively. *$P < 0.05$ *vs* BM. (C and D) Dashed line shows upper normal limit.

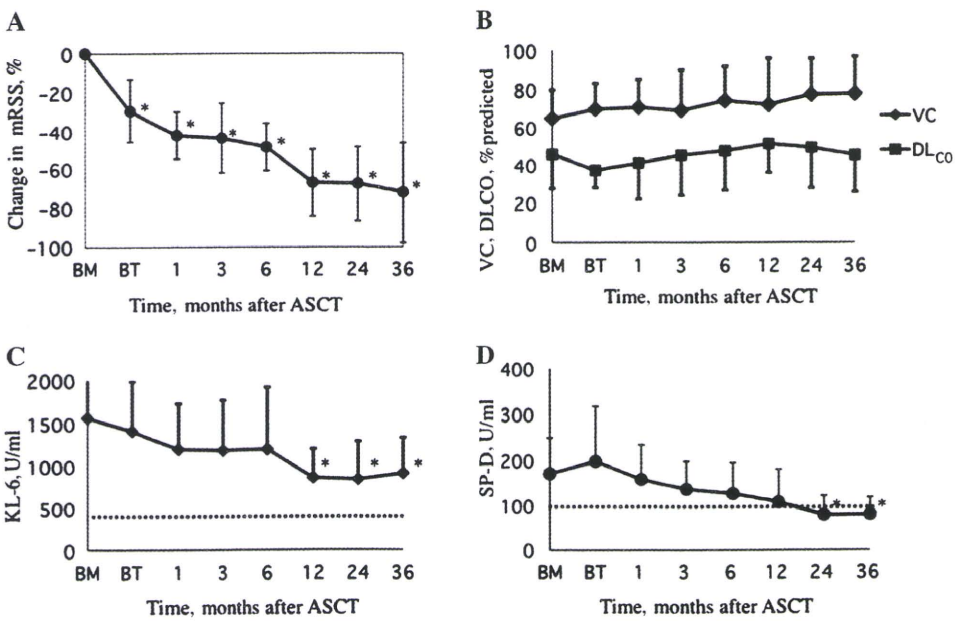

FIG. 2 Evaluation of autoantibody and immunoglobulin. (**A**) Change in the titre of anti-Scl-70. (**B**) Change in the serum levels of IgG, IgA and IgM. Data are presented as mean (S.D.). The *x*-axis is not drawn to scale. The data obtained before mobilization and just before transplantation (HSCT) are shown as BM and BT, respectively. $*P < 0.05$ *vs* BM.

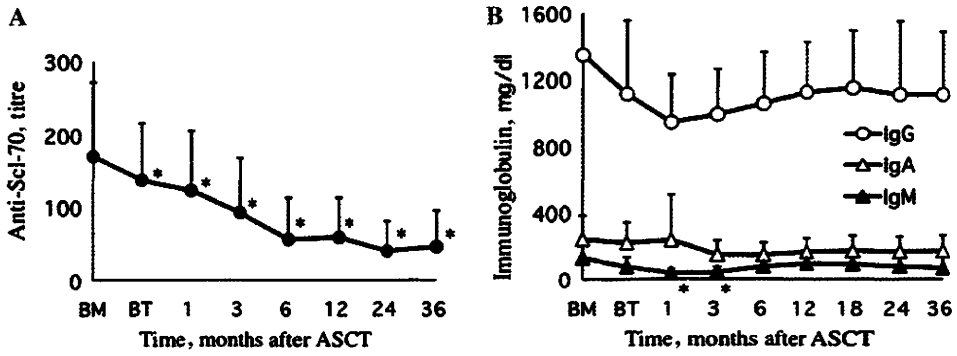

FIG. 3 Kinetics of immunological markers in SSc patients who received ASCT. Data are mean (S.D.). The *x*-axis is not drawn to scale. (**A**) TNF-α, (**B**) TGF-β, (**C**) IL-6, (**D**) sIL-R. The data obtained before mobilization and just before transplantation (HSCT) are shown as BM and BT, respectively. $*P < 0.05$ *vs* BM. Dashed line shows upper normal limit.

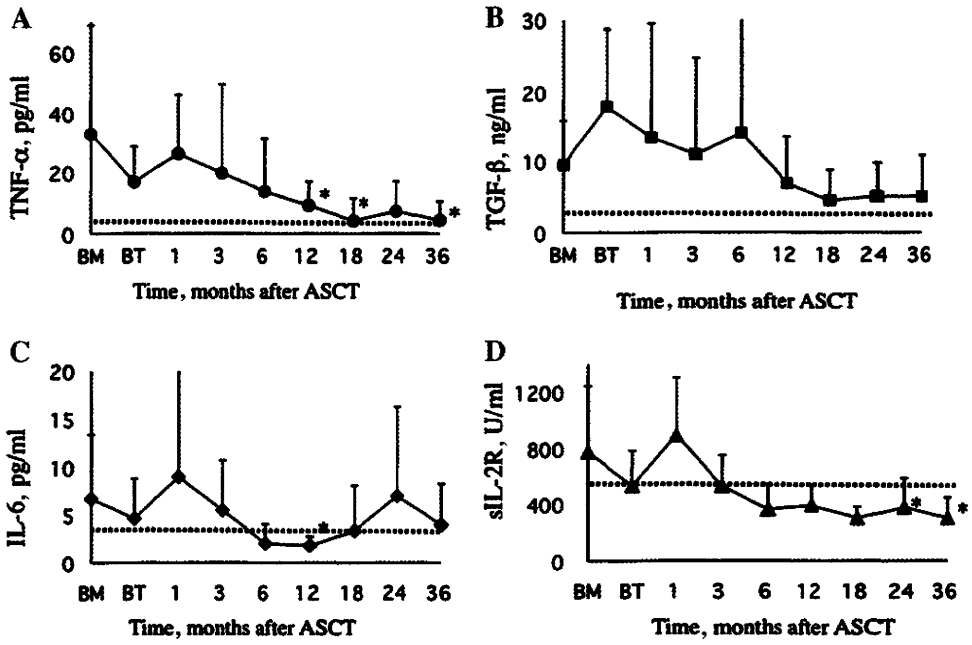

To study whether correction of abnormalities in functional subsets of B cells was associated with durable remission, we focused on the functional subset of $CD19^+$ B cells. The number of $CD19^+CD27^+$ memory B cells was low at baseline, which was characteristic of SSc [23]. An increase in the number of memory B cells, however, was not observed even at 36 months after ASCT, and the vast majority of recovered B cells were naïve $CD19^+CD27^-$B cells (Fig. 4D).

Th1 $CD4^+$ T cells were predominantly reconstituted after $CD34^+$ ASCT

Previous data showed that Th1/Th2 balance was associated with skin sclerosis in an animal model of SSc [15]. Therefore, we analysed Th1/Th2 balance after ASCT by measuring the ratio of intracellular IFN-γ^+/IL-4^-/$CD4^+$ to IFN-γ^-/IL-4^+/$CD4^+$ T cells (Fig. 5). In Fig. 5A, the results of Case 9 before mobilization, 3 and 24 months after HSCT were shown as representative data. IFN-γ^+/IL-4^-/$CD4^+$ and IFN-γ^-/IL-4^+/$CD4^+$ T cells were considered to be Th1 and Th2 cells, respectively. In this case, elimination of IL-4^+/$CD4^+$ (Th2) T cells as well as predominant reconstitution of IFN-γ^+/$CD4^+$ (Th1) T cells were observed after ASCT. The ratio of IFN-γ^+ to IL-4^+ $CD4^+$ T cells was increased from 4.3 before mobilization to 32.8 at 3 months and 197.3 at 24 months after HSCT. When Th1/Th2 balance was analysed in all SSc patients, the ratio of IFN-γ^+/ to IL-4^+/$CD4^+$ T cells was significantly